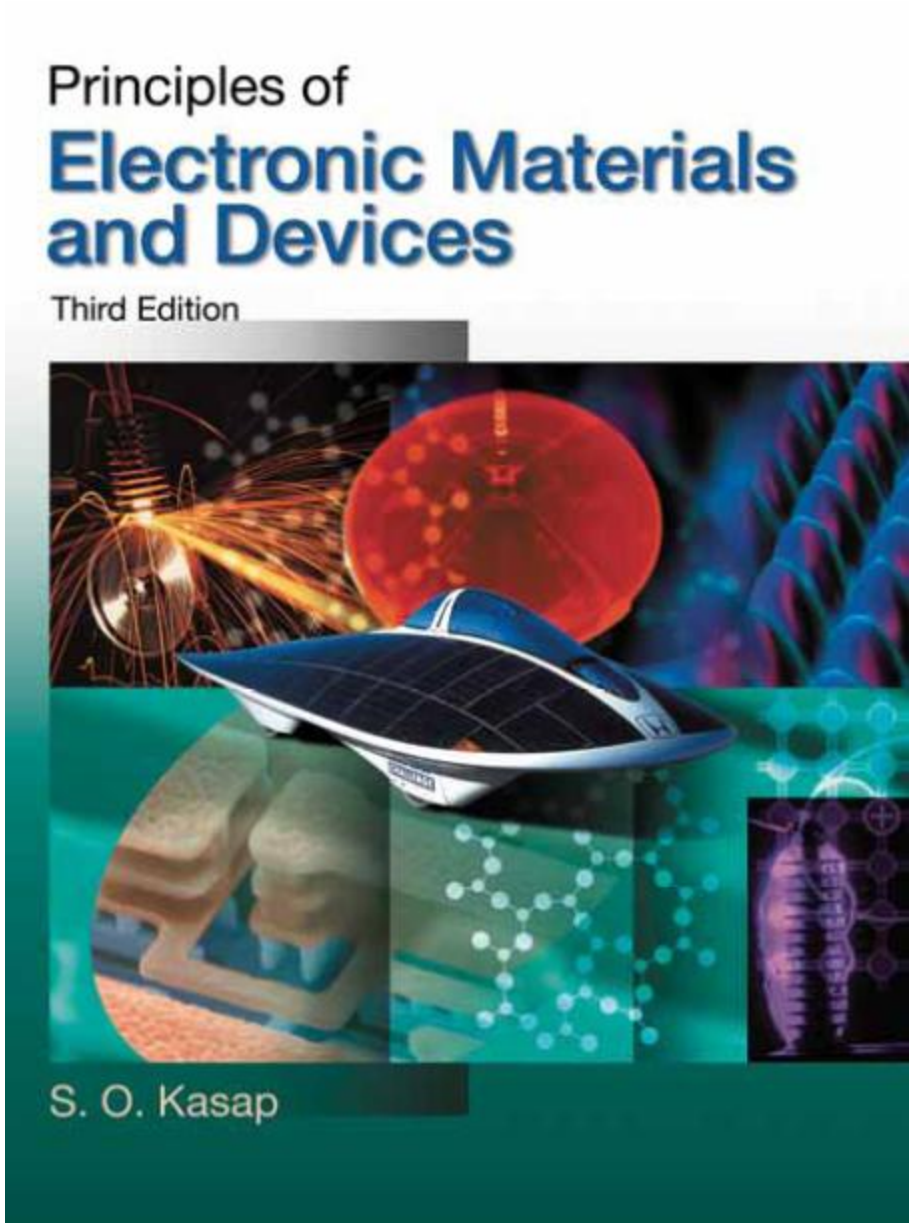

These PowerPoint color diagrams can only be used by instructors if the 3rd Edition has been adopted for his/her course. Permission is given to individuals who have purchased a copy of the third edition with CD-ROM Electronic Materials and Devices to use these slides in seminar, symposium and conference presentations provided that the book title, author and © McGraw-Hill are displayed under each diagram.

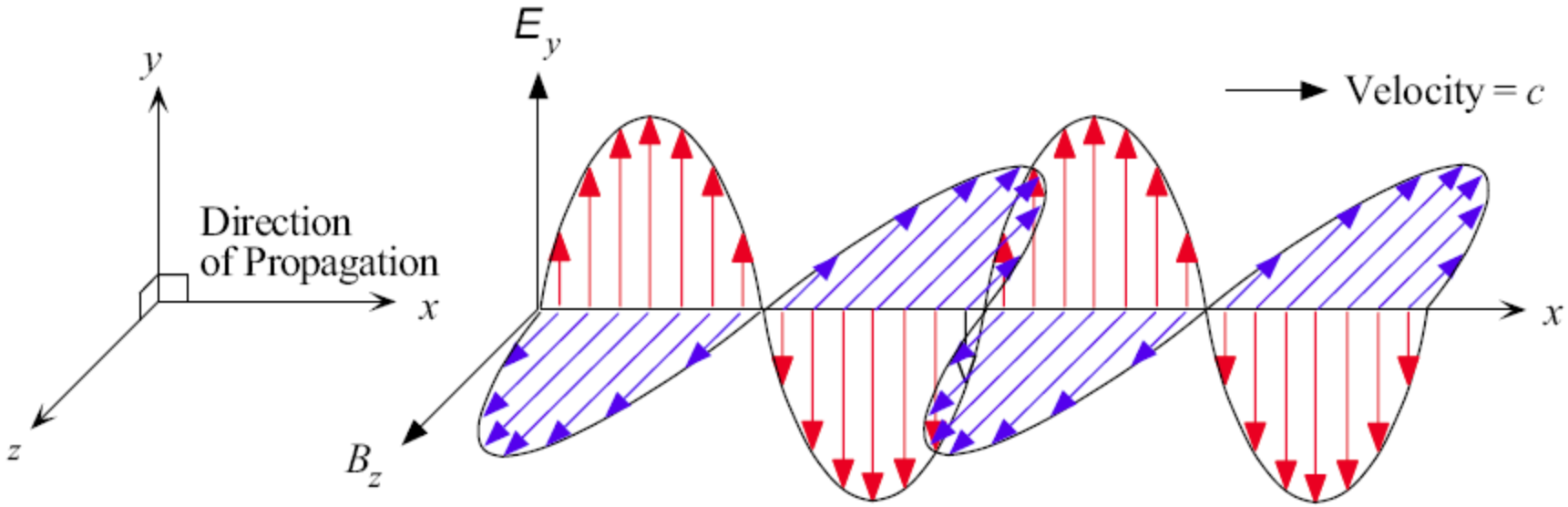

The classical view of light as an electromagnetic wave.
An electromagnetic wave is a traveling wave with time-varying electric and magnetic Fields that are perpendicular to each other and to the direction of propagation.

Fig 3.1

Light as a wave

Traveling wave description

$$\mathcal{E}_y(x,t) = \mathcal{E}_o \sin(kx - \omega t)$$

Intensity of light wave

$$I = \frac{1}{2} c \varepsilon_o \mathcal{E}_o^2$$

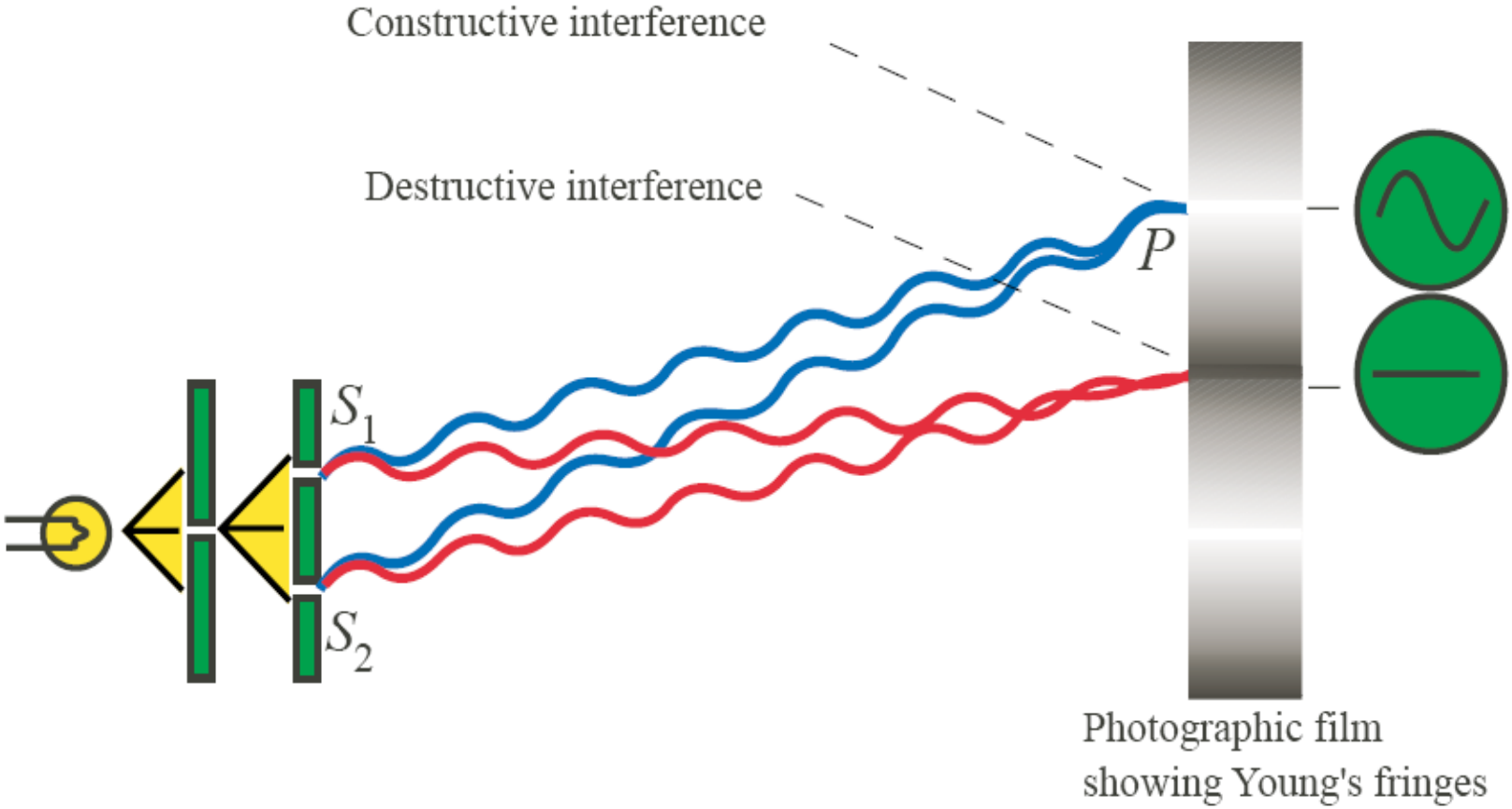

Schematic illustration of Young's double-slit experiment.

Fig 3.2

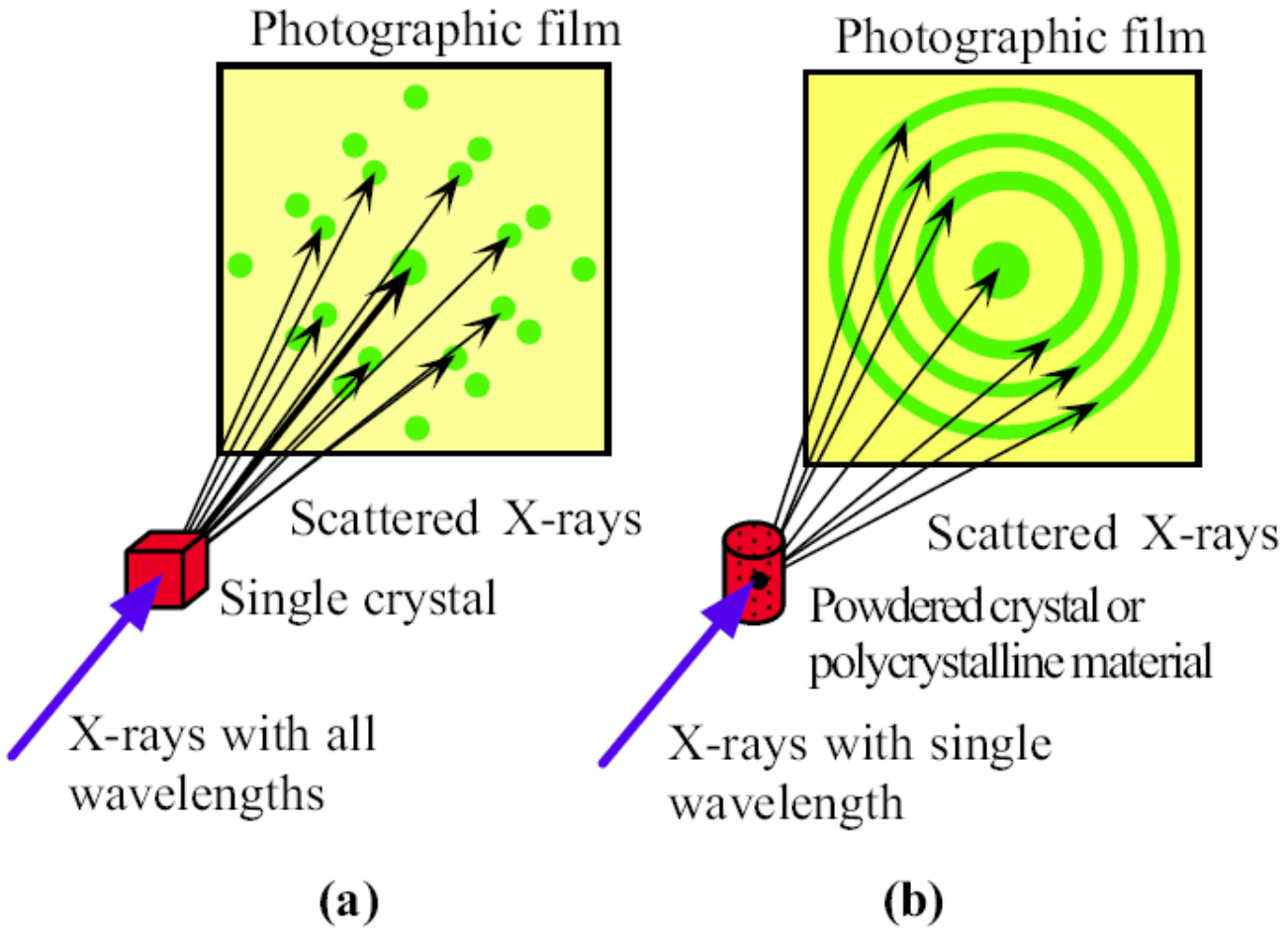

Diffraction patterns obtained by passing X-rays through crystals can only be explained by using ideas based on the interference of waves. (a) Diffraction of X-rays from a single crystal gives a diffraction pattern of bright spots on a photographic film. (b) Diffraction of X-rays from a powdered crystalline material or a polycrystalline material gives a diffraction pattern of bright rings on a photographic film.

Fig 3.3

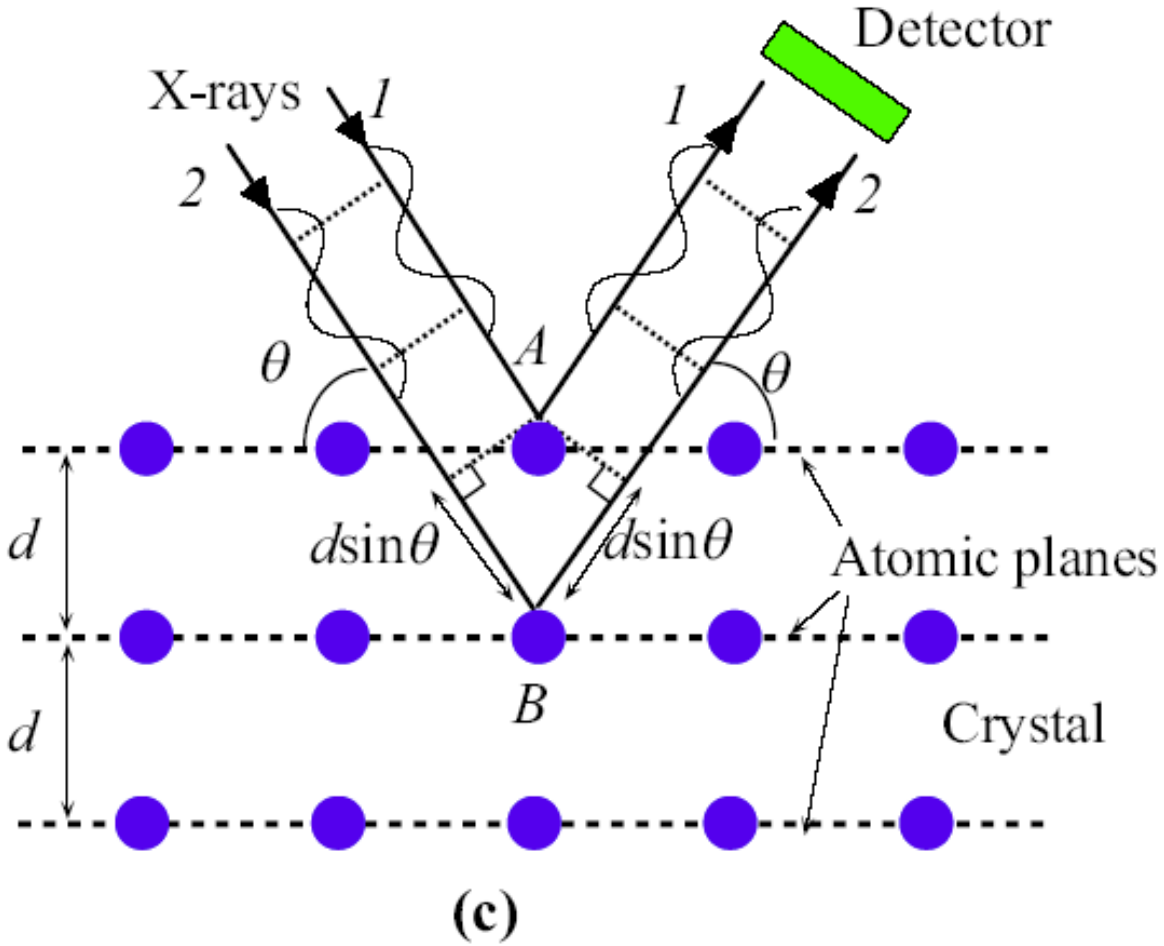

(c) X-ray diffraction involves constructive interference of waves being "reflected" by various atomic planes in the crystal.

Fig 3.3

Bragg's Law

Bragg diffraction condition

$$2d\sin\theta = n\lambda \quad n = 1, 2, 3, \ldots$$

The equation is referred to as **Bragg's law**, and arises from the constructive interference of scattered waves.

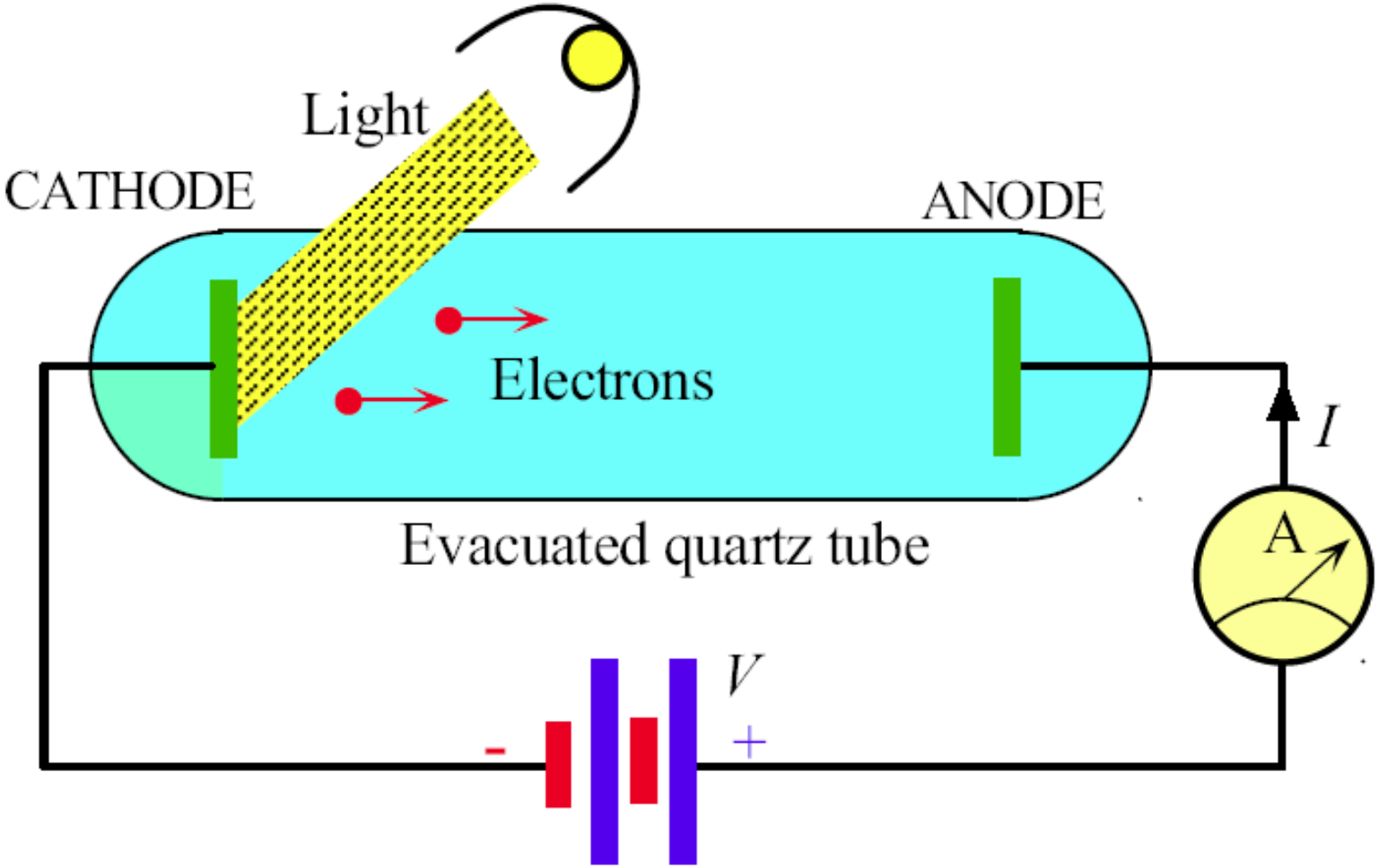

The photoelectric effect.

Fig 3.4

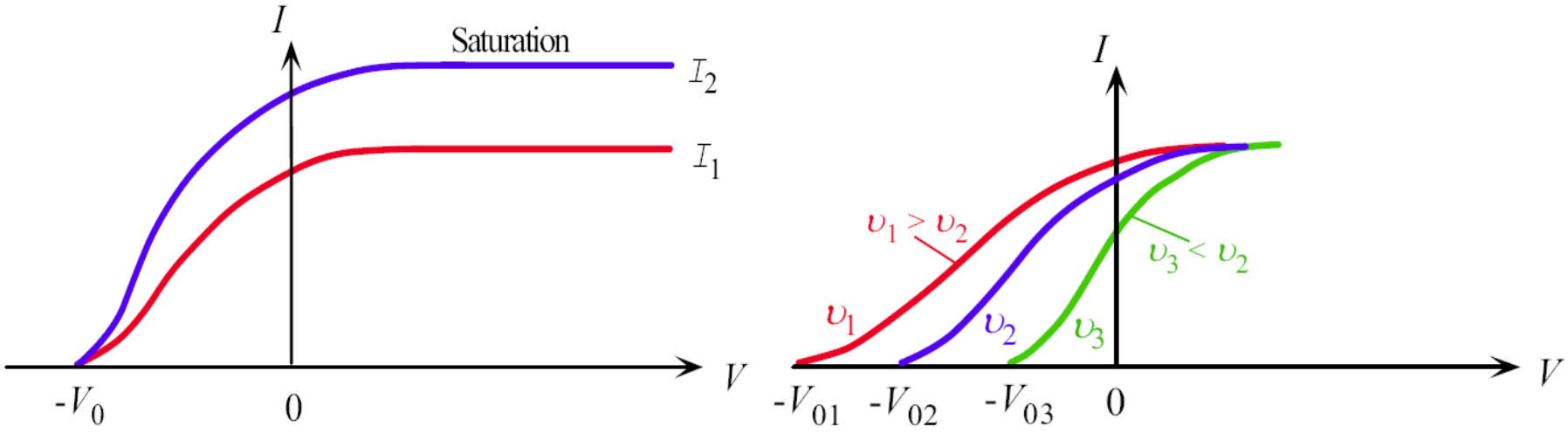

(a) Photoelectric current vs. voltage when the cathode is illuminated with light of identical wavelength but different intensities (I). The saturation current is proportional to the light intensity

(b) The stopping voltage and therefore the maximum kinetic energy of the emitted electron increases with the frequency of light υ. (Note: The light intensity is not the same)

Results from the photoelectric experiment.

Fig 3.5

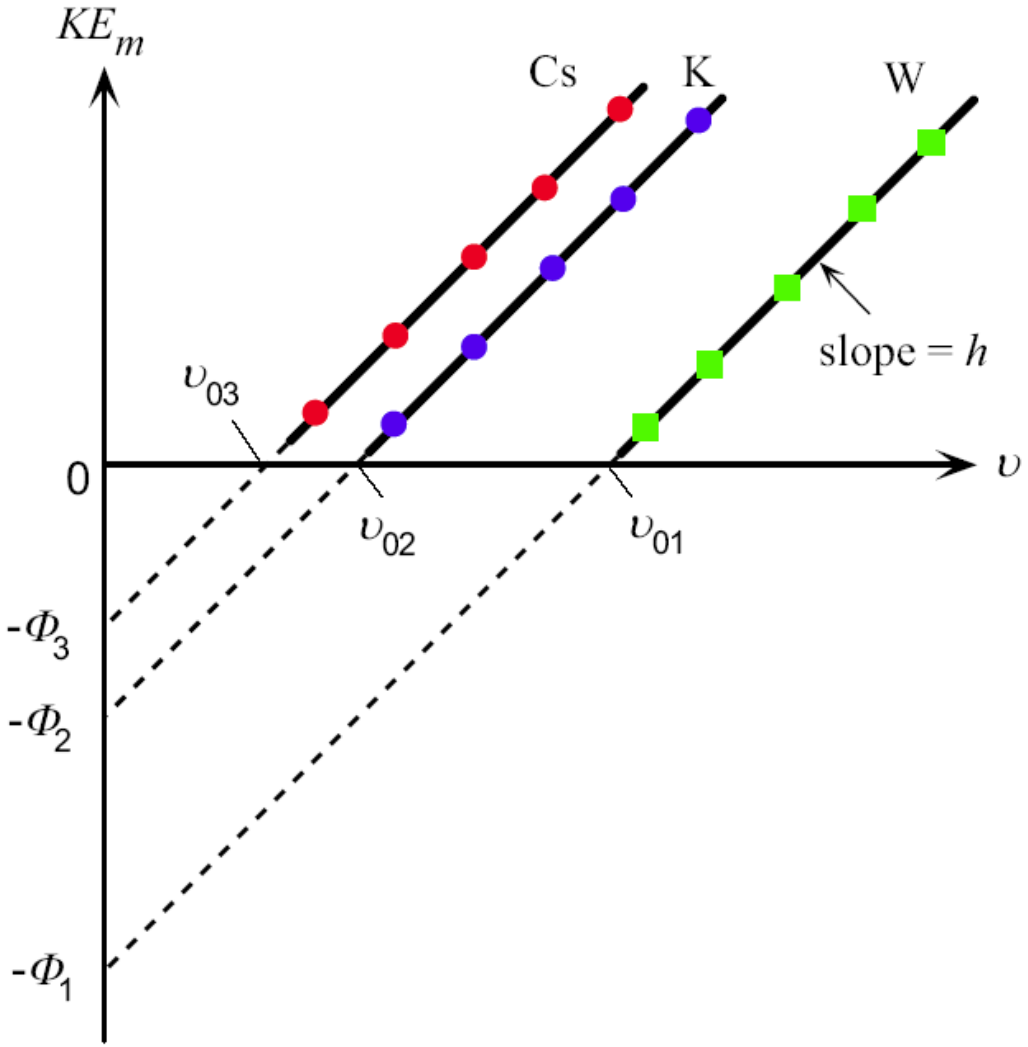

The effect of varying the frequency of light and the cathode material in the photoelectric Experiment. The lines for the different materials have the same slope *h* but different intercepts

Fig 3.6

Photoelectric Effect

Photoemitted electron's maximum *KE* is KE_m

$$KE_m = h\upsilon - h\upsilon_0$$

Work function, Φ_0

The constant *h* is called **Planck's constant**.

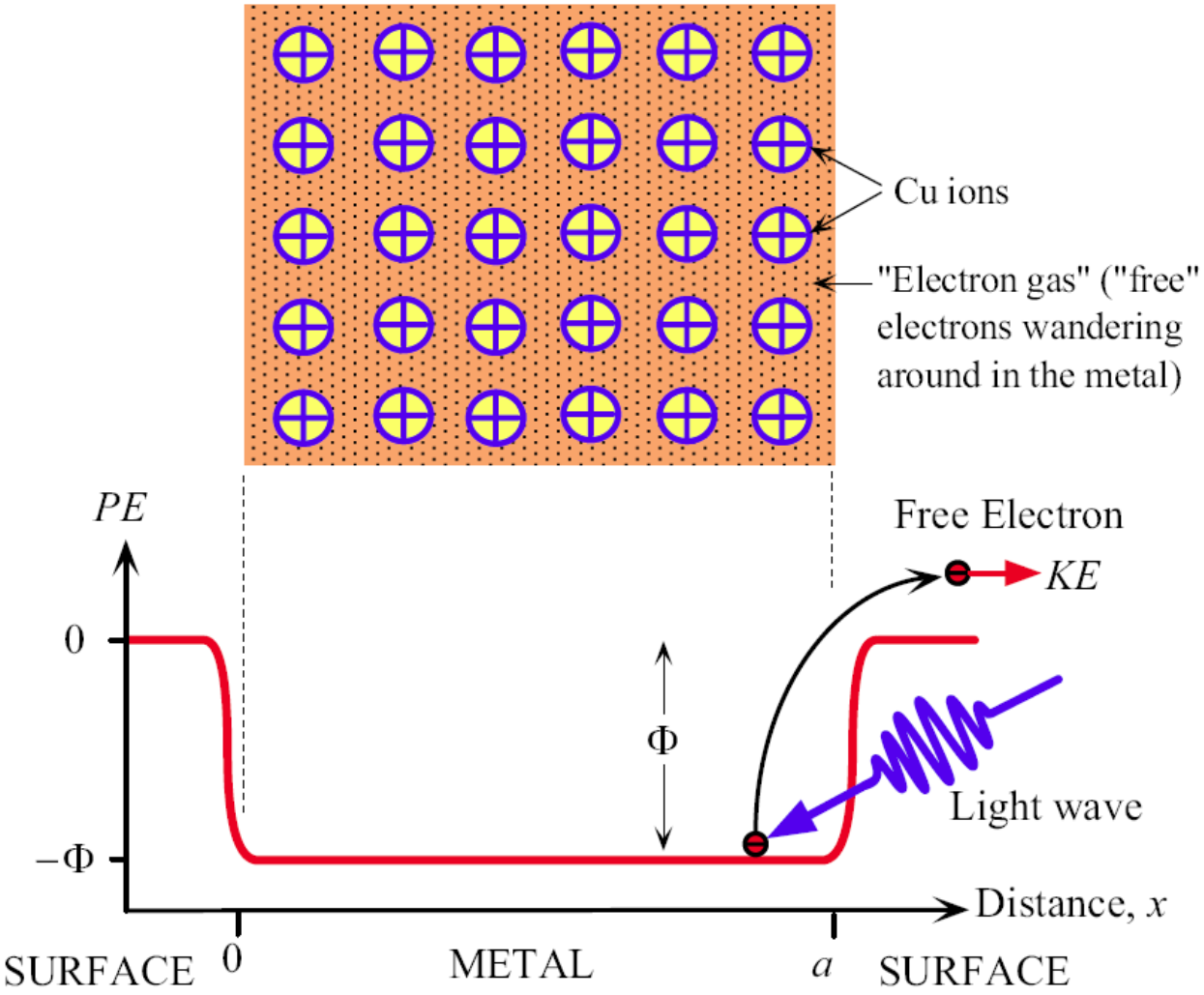

The PE of an electron inside the metal is lower than outside by an energy called the workfunction of the metal. Work must be done to remove the electron from the metal.

Fig 3.7

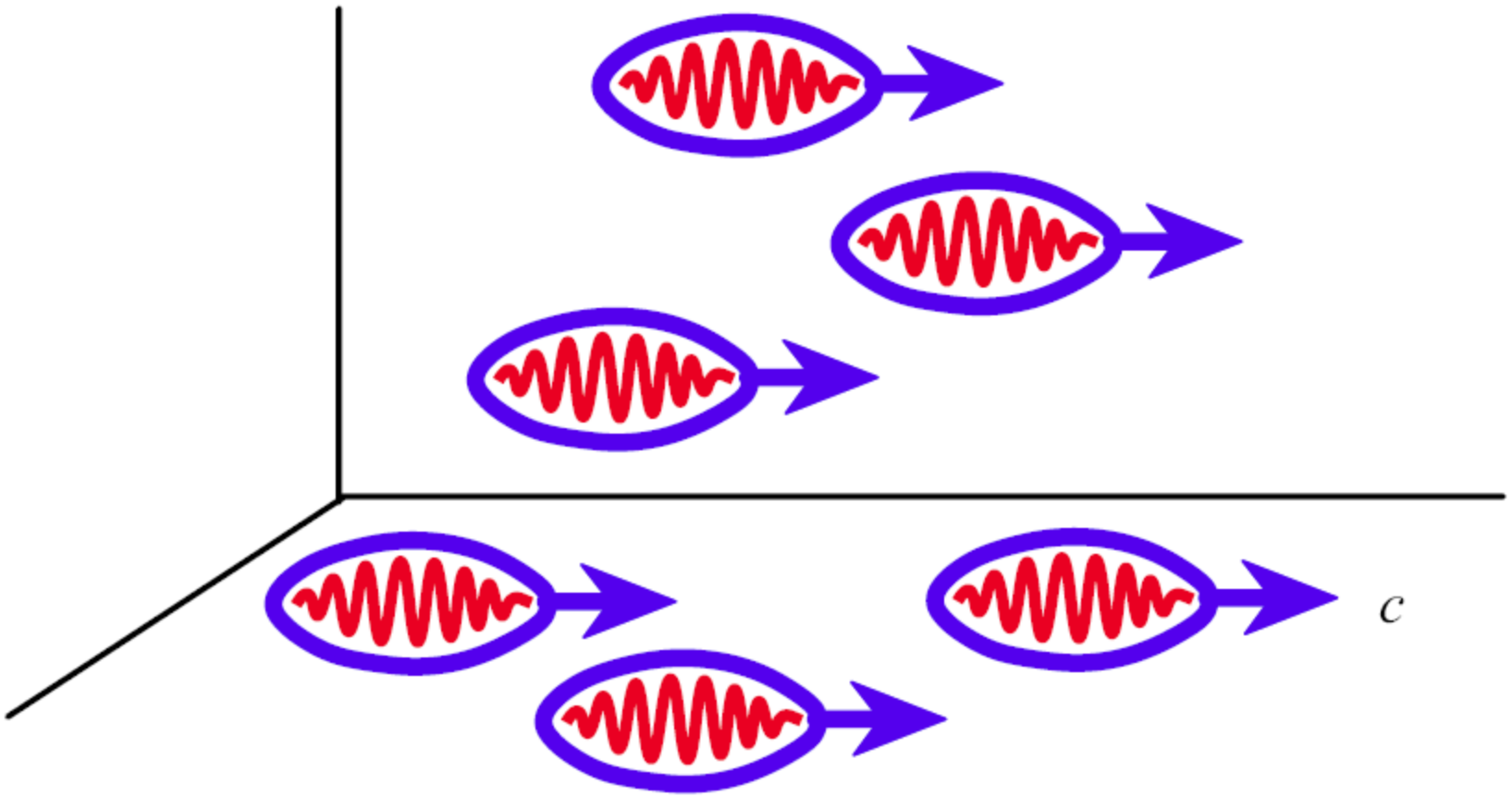

Intuitive visualization of light consisting of a stream of photons (not to be taken too literally).
SOURCE: R. Serway, C. J. Moses, and C. A. Moyer, Modern Physics, Saunders College Publishing, 1989, p. 56, figure 2.16 (b).

Fig 3.8

Light Intensity (Irradiance)

Classical light intensity

$$I = \frac{1}{2} c \varepsilon_o \mathcal{E}_o^2$$

Light Intensity

$$I = \Gamma_{\text{ph}} h\upsilon$$

Photon flux

$$\Gamma_{\text{ph}} = \frac{\Delta N_{\text{ph}}}{A \Delta t}$$

Light consists of photons

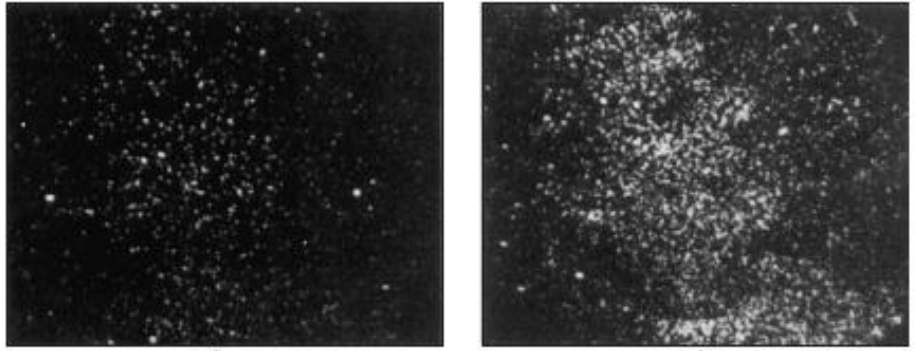

3×10^3 photons

1.2×10^4 photons

9.3×10^4 photons

7.6×10^5 photons

3.6×10^6 photons

2.8×10^7 photons

These electronic images were made with the number of photons indicated. The discrete nature of photons means that a large number of photons are needed to constitute an image with satisfactorily discernable details.

SOURCE: A. Rose, "Quantum and noise limitations of the visual process" *J. Opt. Soc. of America*, vol. 43, 715, 1953. (Courtesy of OSA.)

X-rays are photons

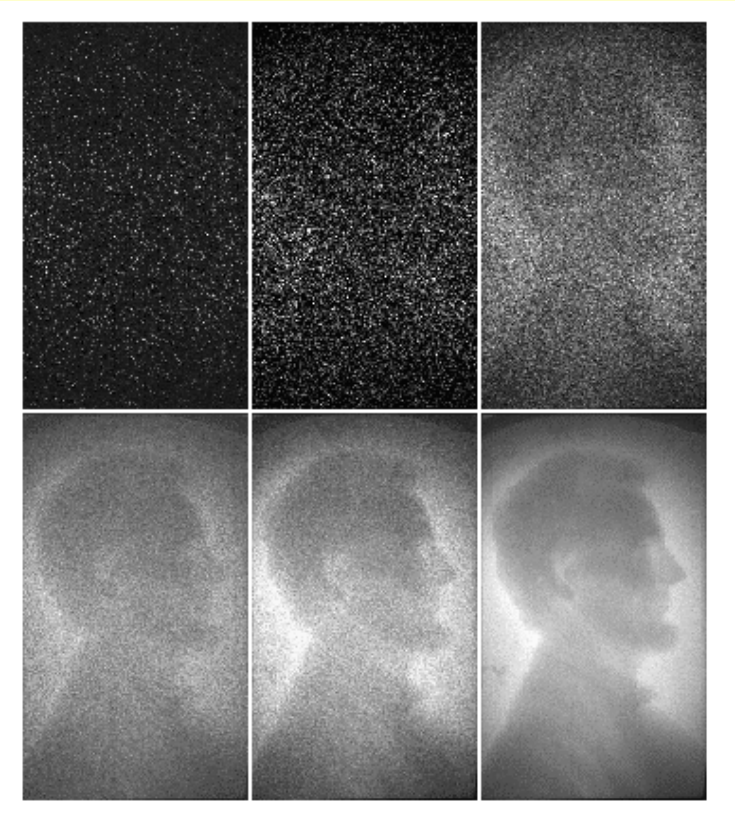

X-ray image of an American one-cent coin captured using an x-ray a-Se HARP camera. The first image at the top left is obtained under extremely low exposure and the subsequent images are obtained with increasing exposure of approximately one order of magnitude between each image. The slight attenuation of the X-ray photons by Lincoln provides the image. The image sequence clearly shows the discrete nature of x-rays, and hence their description in terms of photons.
SOURCE: Courtesy of Dylan Hunt and John Rowlands, Sunnybrook Hospital, University of Toronto.

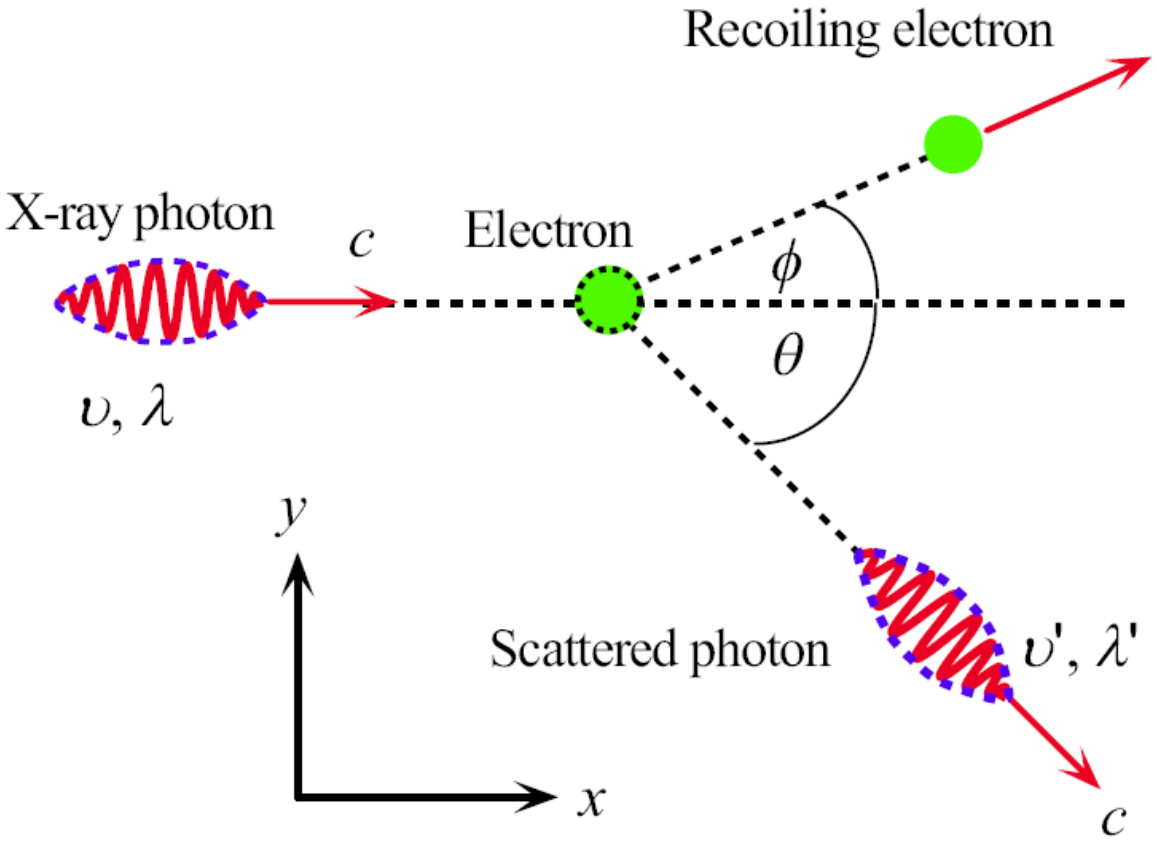

Scattering of an X-ray photon by a “free” electron in a conductor.

Fig 3.9

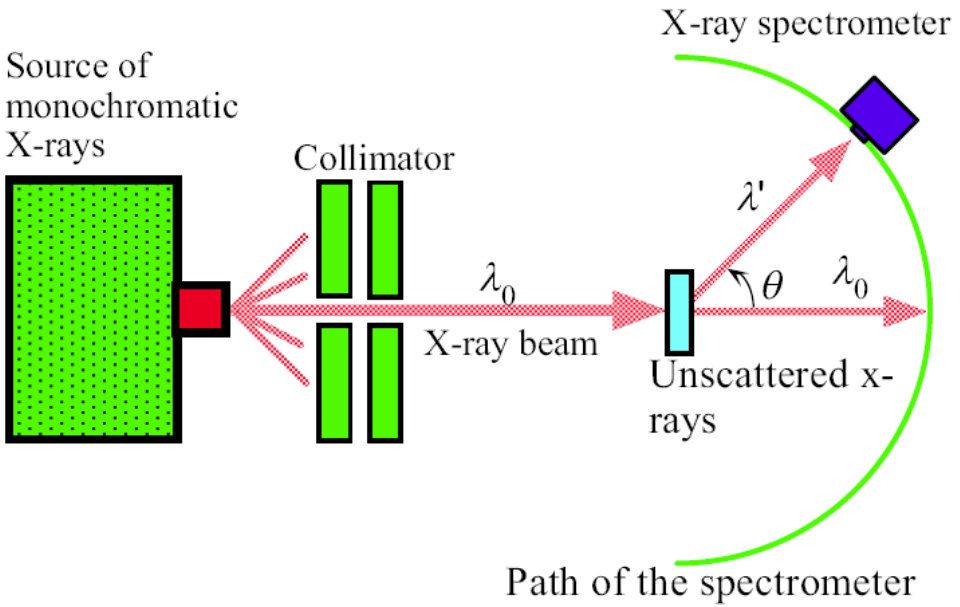

(a) A schematic diagram of the Compton experiment.

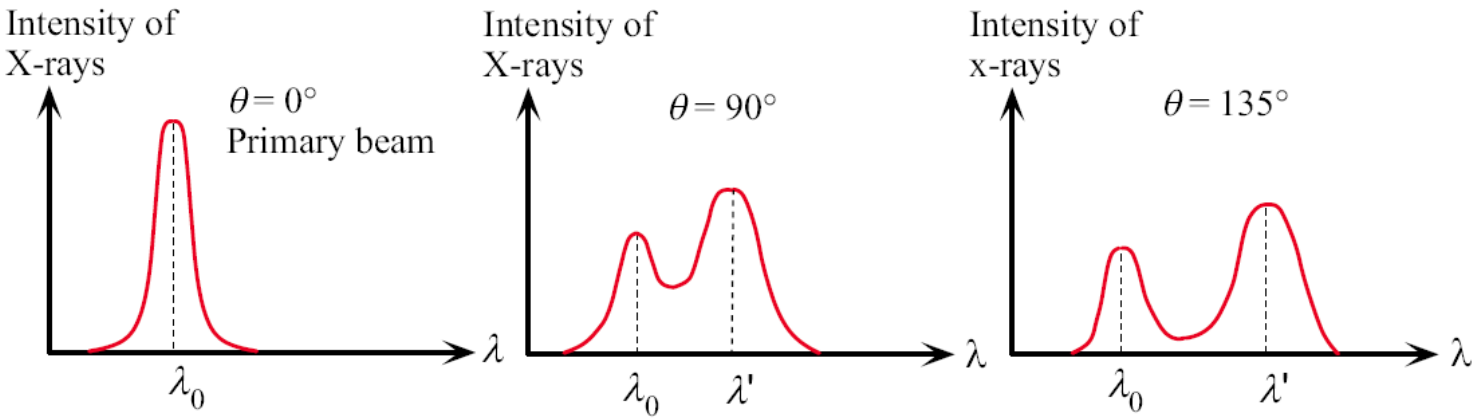

(b) Results from the Compton experiment

The Compton experiment and its results

Fig 3.10

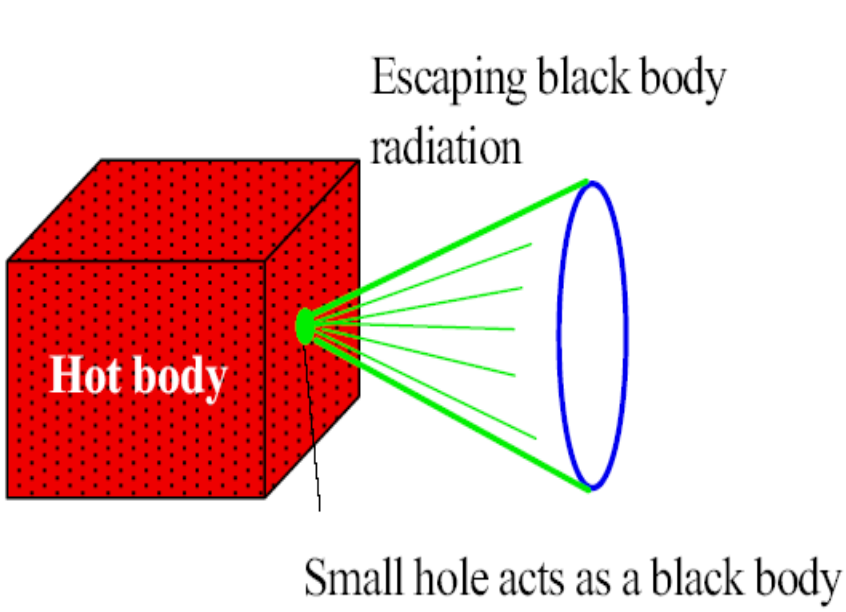

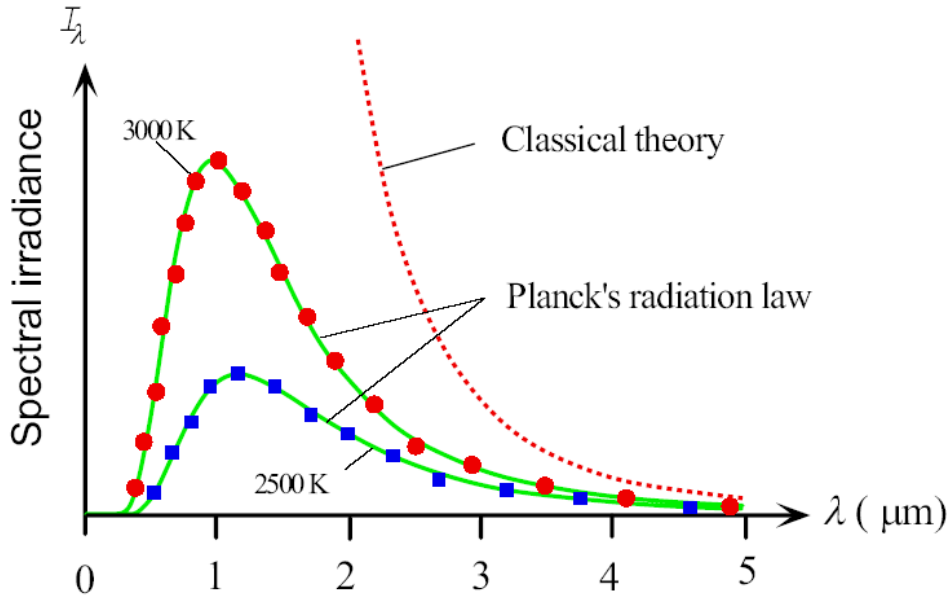

Schematic illustration of black body radiation and its characteristics.
Spectral irradiance vs. wavelength at two temperatures (3000K is about the temperature of The incandescent tungsten filament in a light bulb.)

Fig 3.11

Black Body Radiation

Planck's radiation law

$$I_\lambda = \frac{2\pi hc^2}{\lambda^5\left[\exp\left(\frac{hc}{\lambda kT}\right)-1\right]}$$

Stefan's black body radiation law

$$P_S = \sigma_S T^4$$

Stefan's constant

$$\sigma_S = \frac{2\pi^5 k^4}{15c^2h^3} = 5.670\times10^{-8}\ \mathrm{W\,m^{-2}\,K^{-4}}$$

Stefan's law for real surfaces
Electromagnetic radiation emitted from a hot surface

$P_{\text{radiation}}$ = total radiation power emitted (W = J s^{-1})

$$P_{\text{radiation}} = S\varepsilon\sigma_S[T^4 - T_0^4]$$

σ_S = Stefan's constant, W m^{-2} K^{-4}

ε = emissivity of the surface

$\varepsilon = 1$ for a perfect black body

$\varepsilon < 1$ for other surfaces

S = surface area of emitter (m^2)

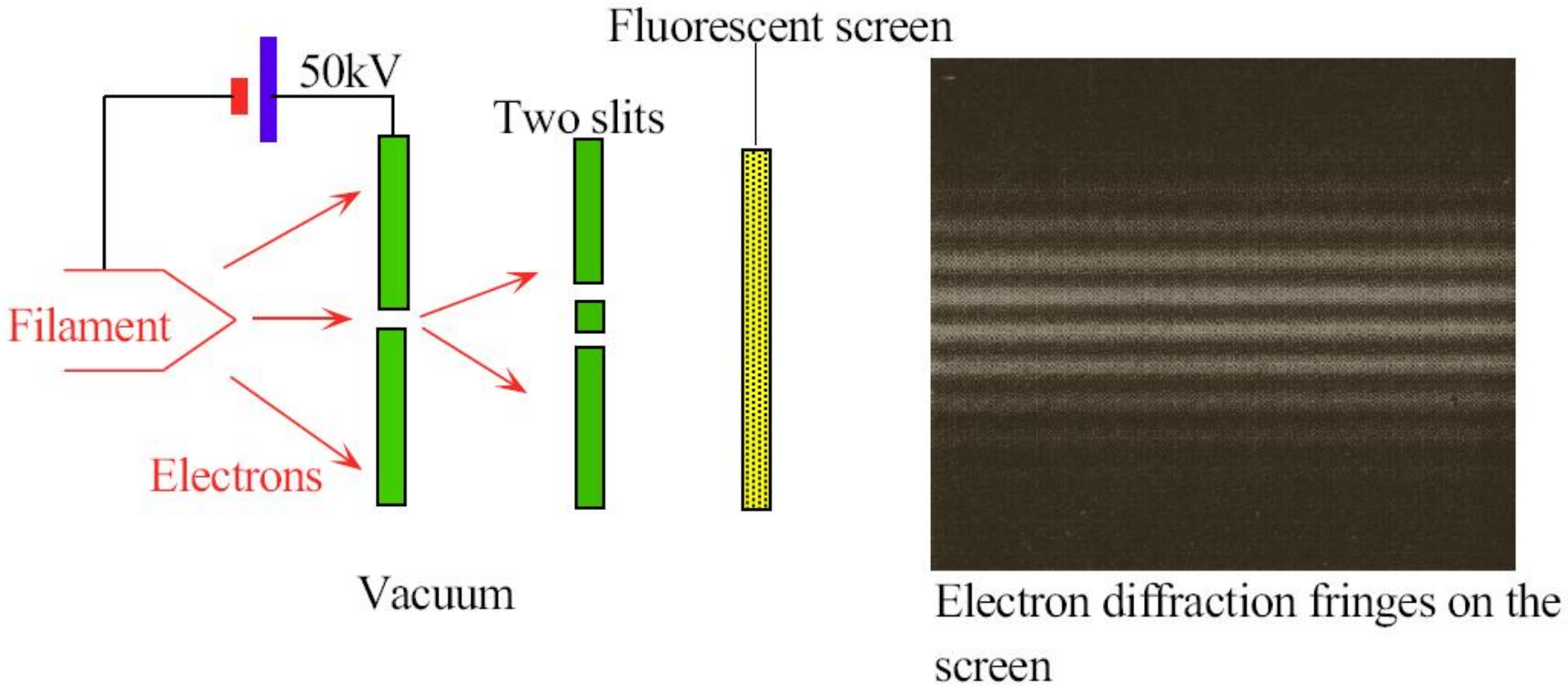

Young's double-slit experiment with electrons involves an electron gun and two slits in a Cathode ray tube (CRT) (hence, in vacuum).
Electrons from the filament are accelerated by a 50 kV anode voltage to produce a beam that Is made to pass through the slits. The electrons then produce a visible pattern when they strike A fluorescent screen (e.g., a TV screen), and the resulting visual pattern is photographed.
SOURCE: Pattern from C. Jonsson, D. Brandt, and S. Hirschi, *Am. J. Physics*, 42, 1974, p.9, figure 8. Used with permission.

Fig 3.12

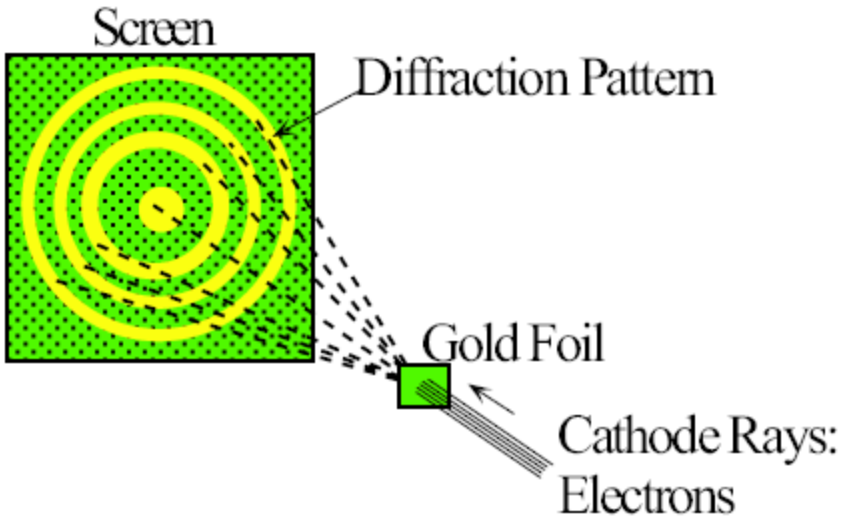

(a) Thomson diffracted electrons by using a thin gold foil and produced a diffraction pattern on the screen of his apparatus in (b). The foil was polycrystalline so that the diffraction pattern was circular rings.

Fig 3.13

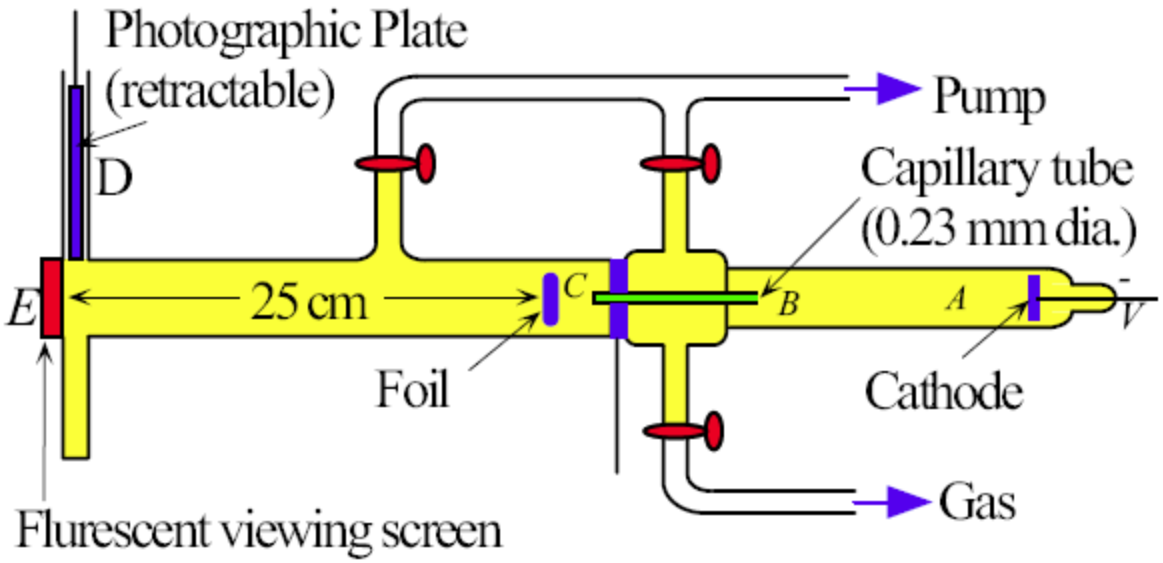

(b): Thomson's electron diffraction apparatus. A beam of electrons is generated in tube *A*, passed through collimating tube *B*, and made to impinge on a thin gold foil C. The transmitted electrons impinge on the fluorescent screen *E*, or a photographic plate *D* which could be lowered into the path. The entire apparatus was evacuated during the experiment (after G.P. Thompon, Proceedings of the Royal Society, A117 600 (1928)).

Fig 3.13

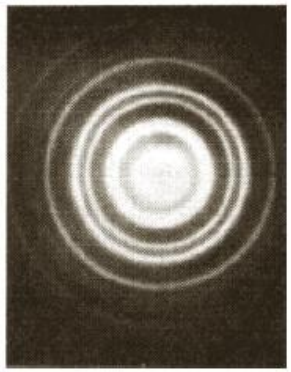

(c) Electron diffraction pattern obtained by G. P. Thomson using a gold foil target.

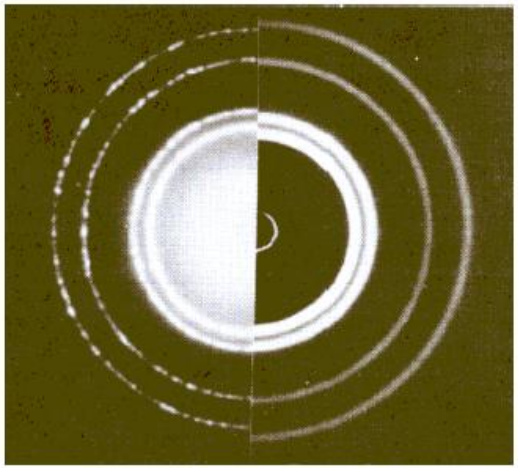

(d) Composite photograph showing diffraction patterns produced with an aluminum foil by X-rays and electrons of similar wavelength. Left: X-rays of $\lambda = 0.071$ nm. Right: Electrons of energy 600 eV.

(e)

(e) Diffraction pattern produced by 40 keV electrons passing through zinc oxide powder. The distribution of the pattern was produced by a small magnet which was placed between the sample and the photographic plate. An X-ray diffraction pattern would not be affected by a magnetic field.

The diffraction of electrons by crystals gives typical diffraction patterns that would be Expected if waves being diffracted as in x-ray diffraction with crystals [(c) and (d) from A. P. French and F. Taylor, *An Introduction to Quantum Mechanics* (Norton, New York, 1978), p. 75; (e) from R. B. Leighton, *Principles of Modern Physics*, McGraw-Hill, 1959), p. 84.

Fig 3.13

De Broglie Relationship

Wavelength λ of the electron depends on its momentum p

$$\lambda = \frac{h}{p}$$

De Broglie relations

$$\lambda = \frac{h}{p} \qquad \text{OR} \qquad p = \frac{h}{\lambda}$$

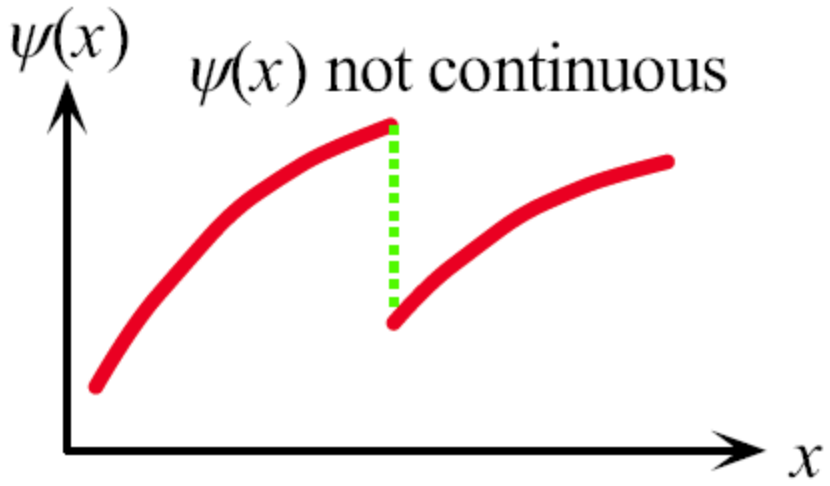

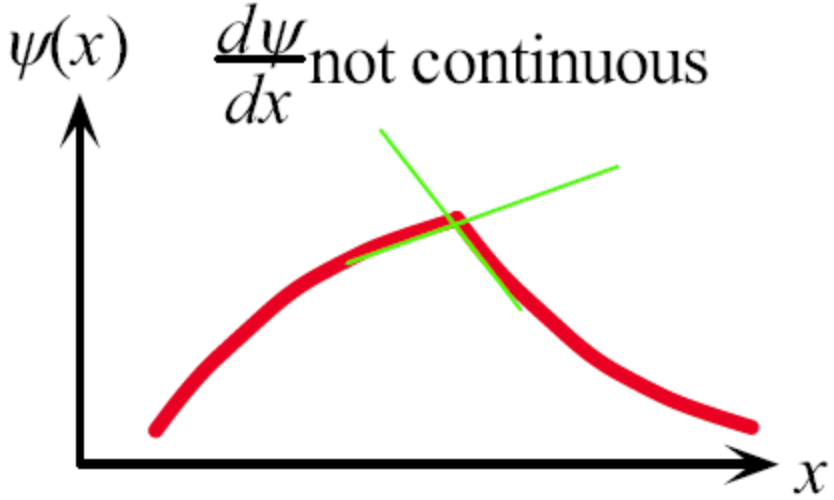

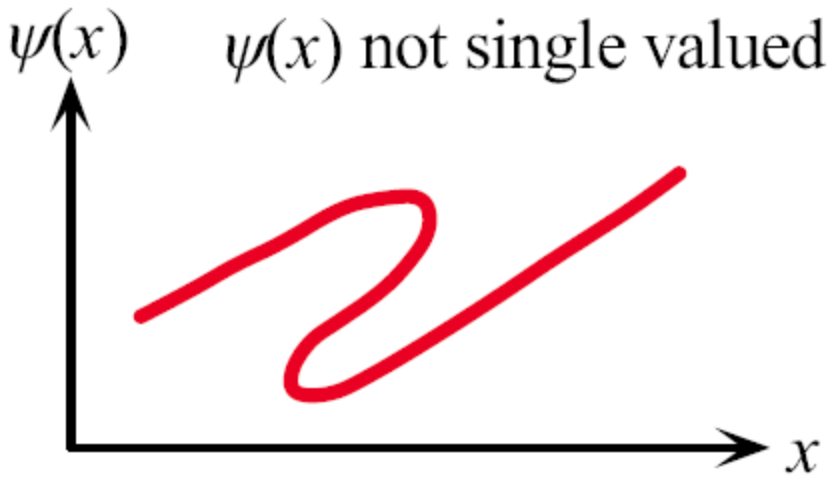

Unacceptable forms of $\psi(x)$

Fig 3.14

Time-Independent Schrodinger Equation

Steady-state total wave function

$$\Psi(x,t) = \psi(x)\exp\left(-\frac{jEt}{\hbar}\right)$$

Schrodinger's equation for one dimension

$$\frac{d^2\psi}{dx^2} + \frac{2m}{\hbar^2}(E-V)\psi = 0$$

Schrondinger's equation for three dimensions

$$\frac{\partial^2\psi}{\partial x^2} + \frac{\partial^2\psi}{\partial y^2} + \frac{\partial^2\psi}{\partial z^2} + \frac{2m}{\hbar^2}(E-V)\psi = 0$$

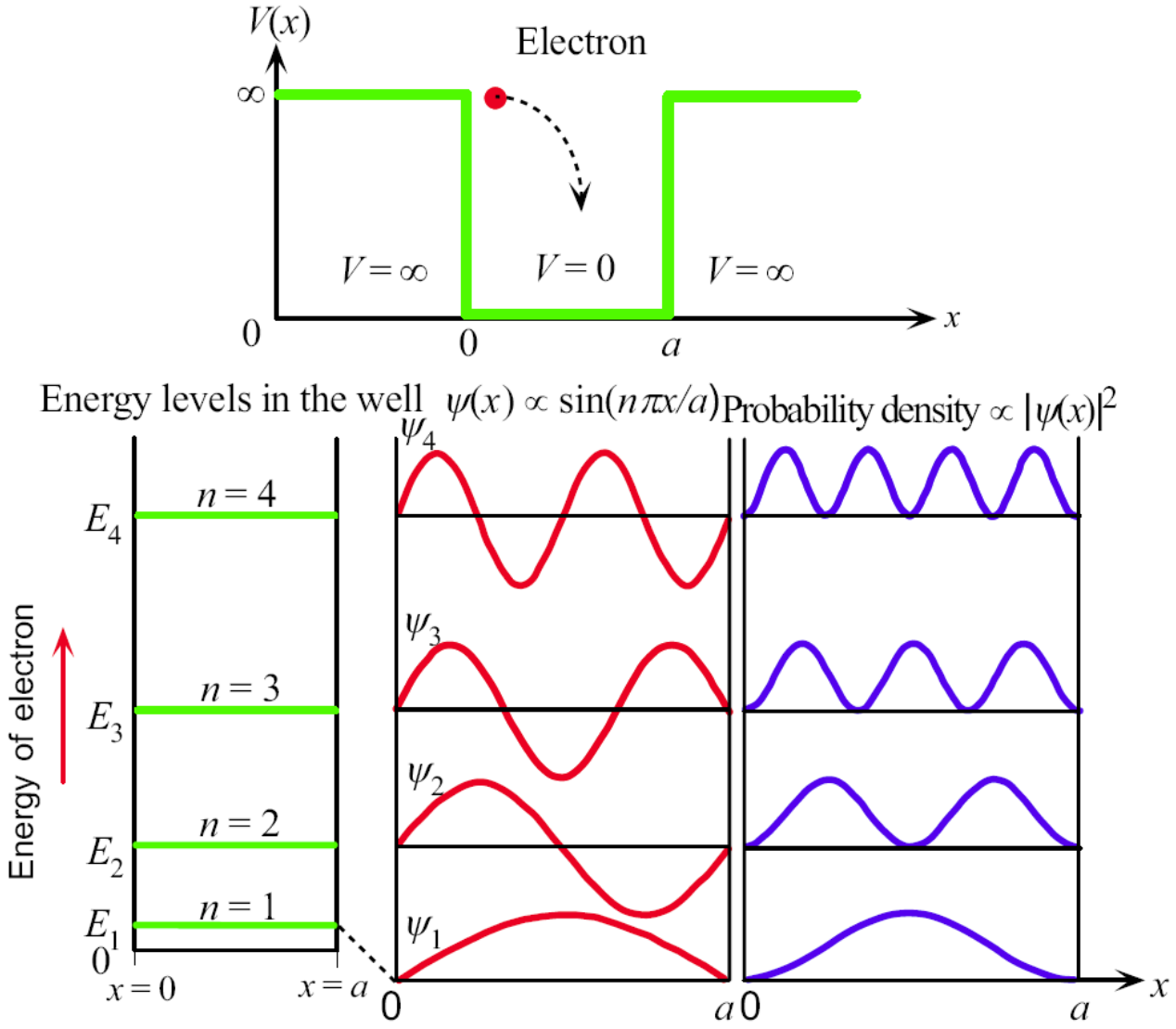

Electron in a one-dimensional infinite PE well.
The energy of the electron is quantized. Possible wavefunctions and the probability distributions for the electron are shown. Fig 3.15

Infinite Potential Well

Wavefunction in an infinite PE well

$$\psi_n(x) = 2Aj \sin\left(\frac{n\pi x}{a}\right)$$

Electron energy in an infinite PE well

$$E_n = \frac{\hbar^2(\pi n)^2}{2ma^2} = \frac{h^2 n^2}{8ma^2}$$

Energy separation in an infinite PE well

$$\Delta E = E_{n+1} - E_n = \frac{h^2(2n+1)}{8ma^2}$$

Heisenberg's Uncertainty Principle

Heisenberg uncertainty principle for position and momentum

$$\Delta x \Delta p_x \geq \hbar$$

Heisenberg uncertainty principle for energy and time

$$\Delta E \Delta t \geq \hbar$$

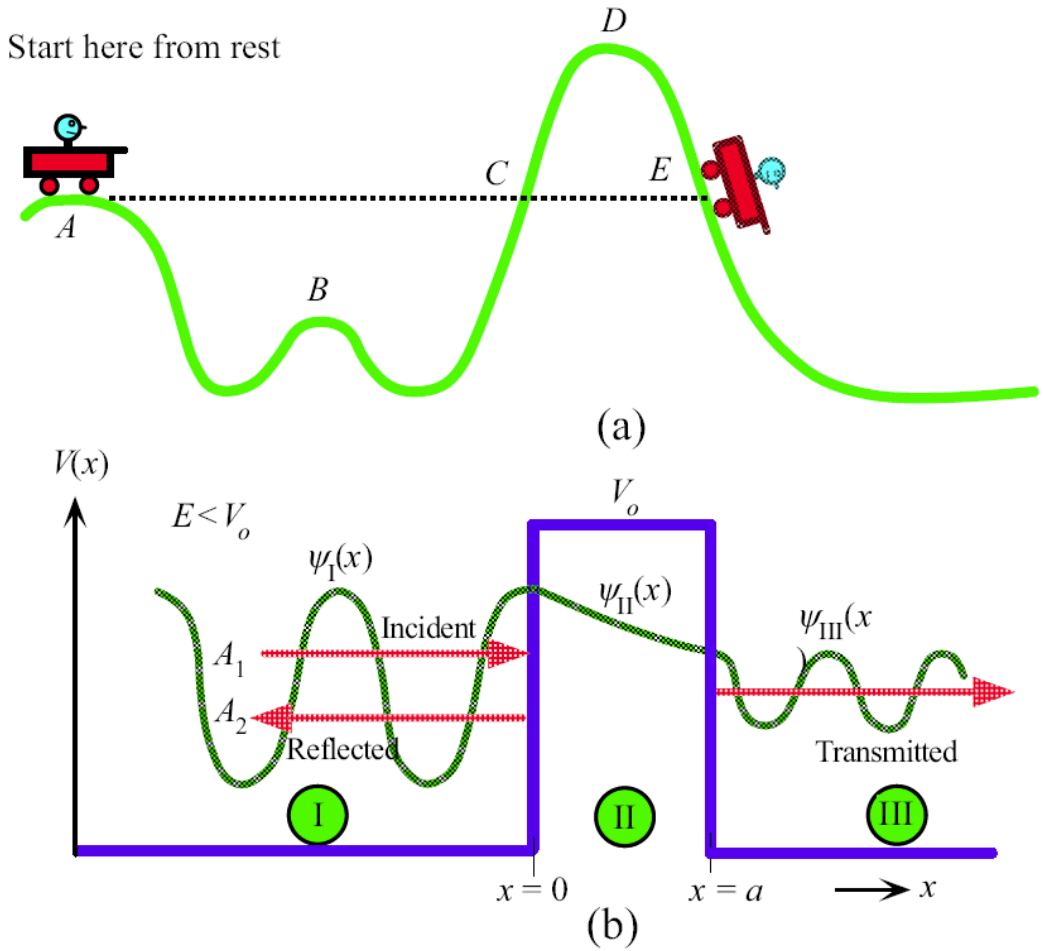

(a) The roller coaster released from *A* can at most make it to *C*, but not to *E*. Its *PE* at *A* is less than the *PE* at *D*. When the car is at the bottom, its energy is totally *KE*. *CD* is the energy barrier that prevents the care from making it to *E*. In quantum theory, on the other hand, there is a chance that the care could tunnel (leak) through the potential energy barrier between *C* and *E* and emerge on the other side of hill at *E*.
(b) The wavefunction for the electron incident on a potential energy barrier (V_0). The incident And reflected waves interfere to give $\psi_1(x)$. There is no reflected wave in region III. In region II, the wavefunction decays with *x* because $E < V_0$.

Fig 3.16

Tunneling Phenomenon: Quantum Leak

Probability of tunneling

$$T = \frac{\left|\psi_{\text{III}}(x)\right|^2}{\left|\psi_{\text{I}}(x)\right|^2} = \frac{C_1^2}{A_1^2} = \frac{1}{1 + D\sinh^2(\alpha a)}$$

Probability of tunneling through

$$T = T_o \exp(-2\alpha a) \quad \text{where} \quad T_o = \frac{16E(V_o - E)}{V_o^2}$$

Reflection coefficient *R*

$$R = \frac{A_2^2}{A_1^2} = 1 - T$$

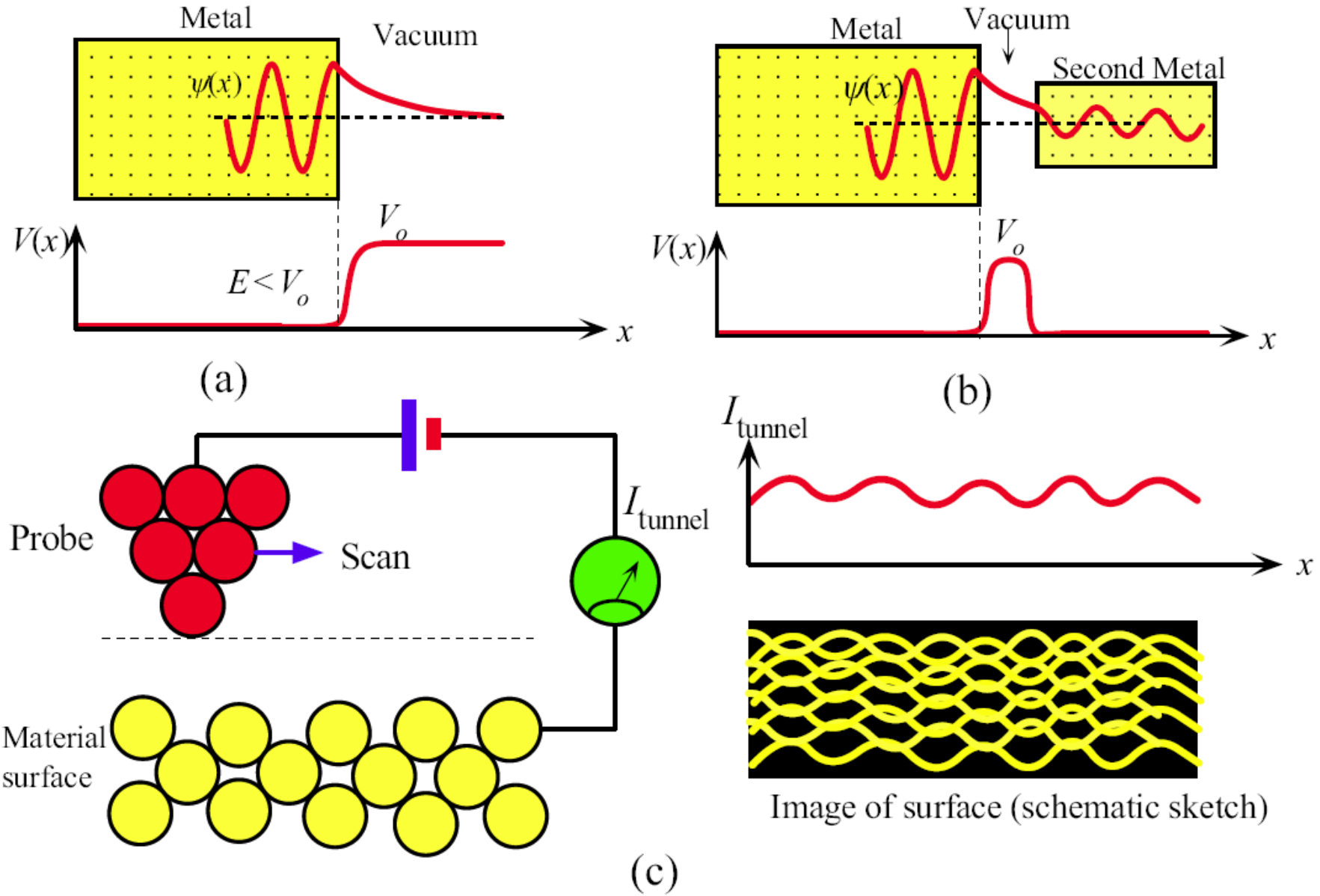

Fig 3.17

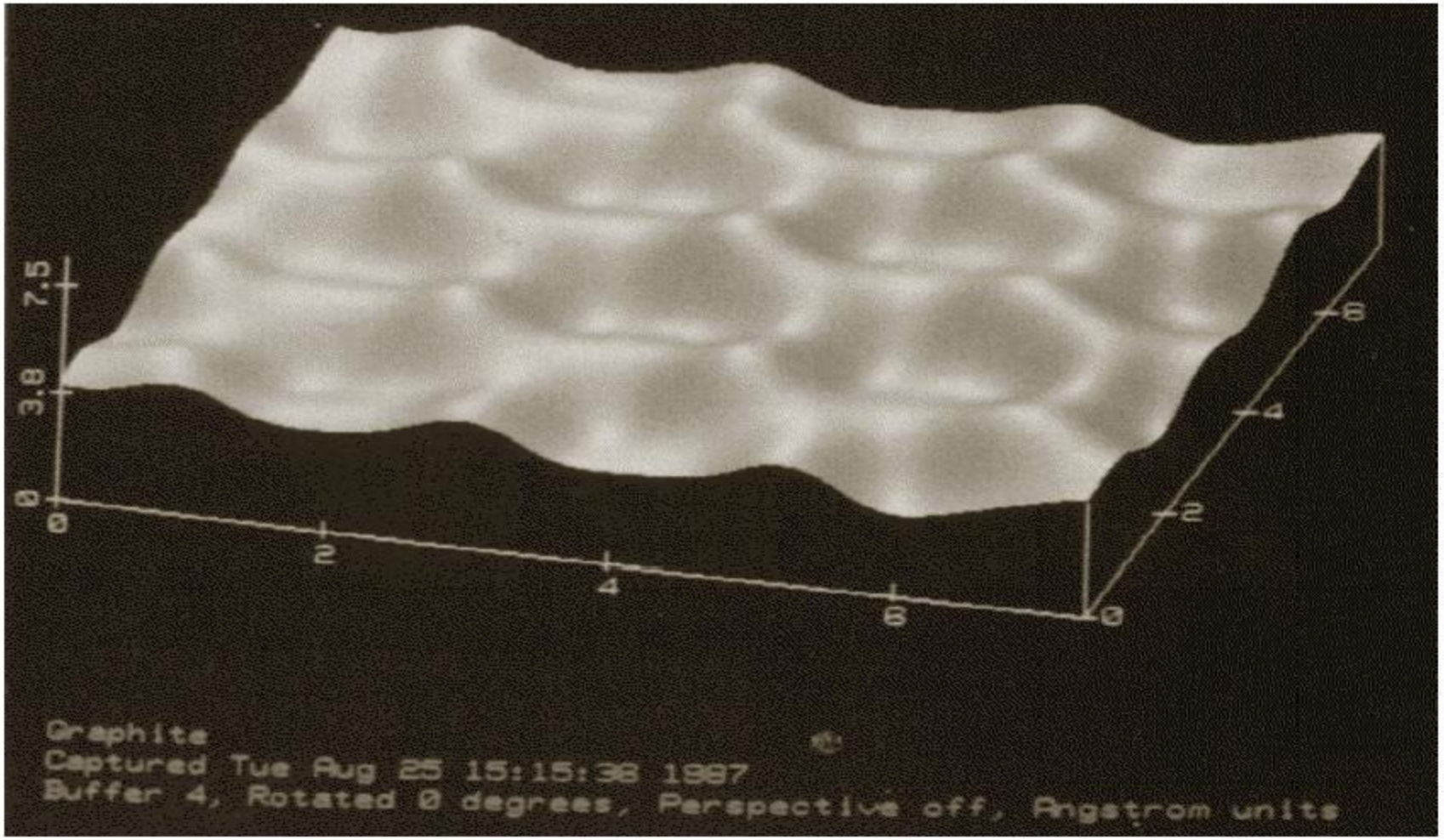

Scanning Tunneling Microscopy (STM) image of a graphite surface where contours represent electron concentrations within the surface, and carbon rings are clearly visible. Two Angstrom scan. |SOURCE: Courtesy of Veeco Instruments, Metrology Division, Santa Barbara, CA.

Fig 3.18

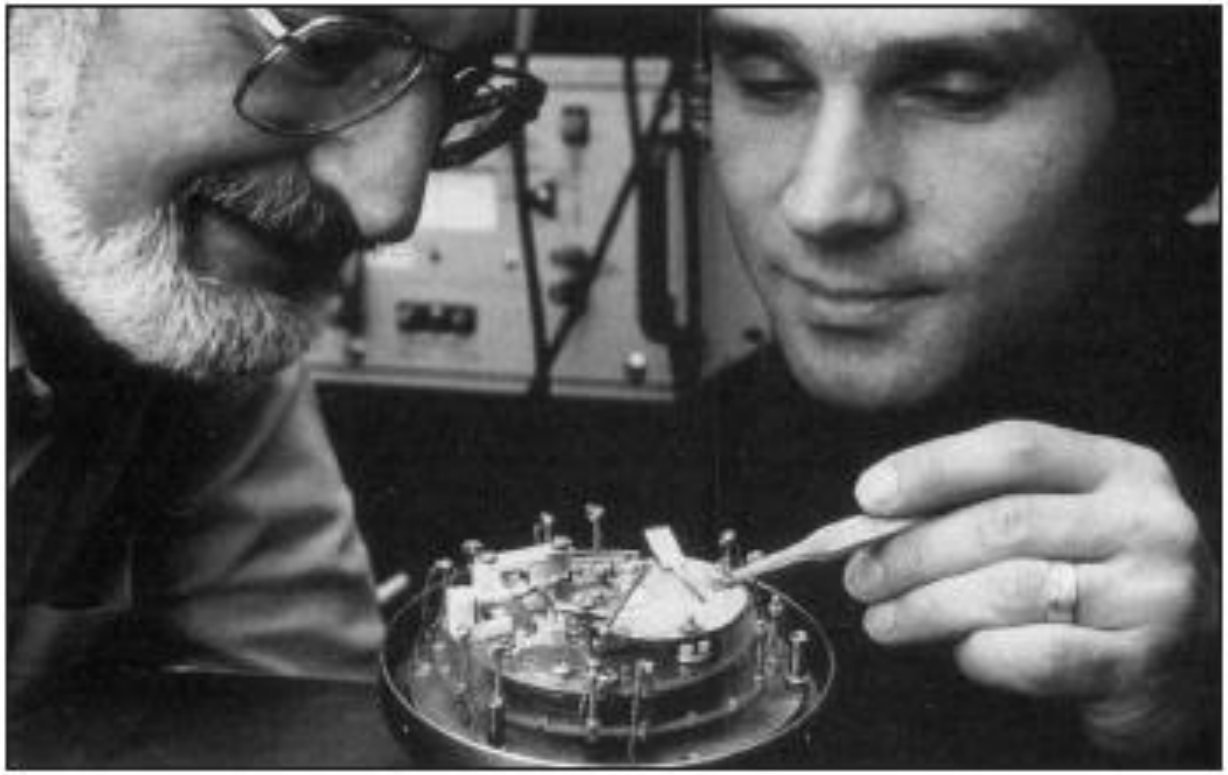

STM's inventors Gerd Binning (right) and Heinrich Rohrer (left), at IBM Zurich Research Laboratory with one of their early devices. They won the 1986 Nobel prize for the STM.

| SOURCE: Courtesy of IBM Zurich Research Laboratory.

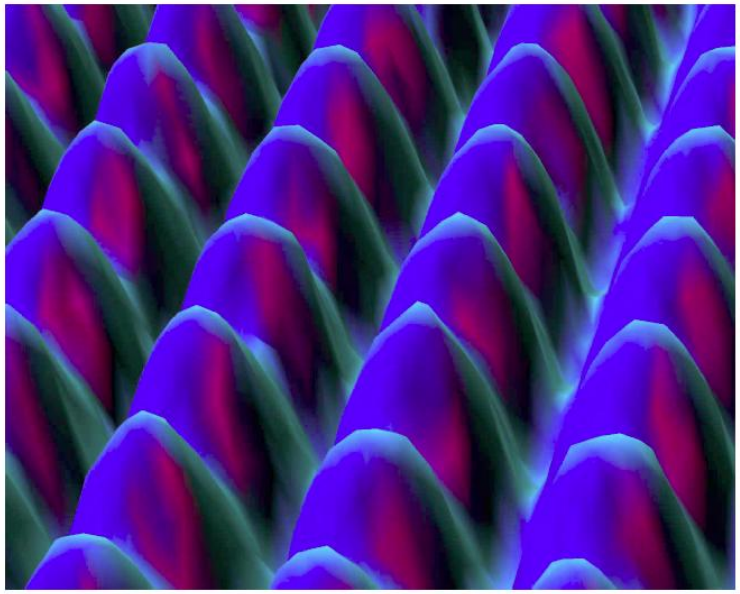

STM image of Ni (100) surface

SOURCE: Courtesy of IBM

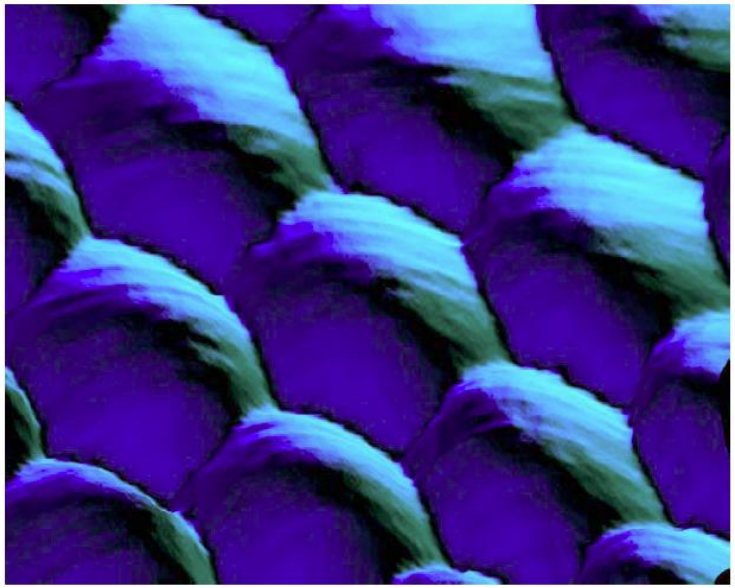

STM image of Pt (111) surface

SOURCE: Courtesy of IBM

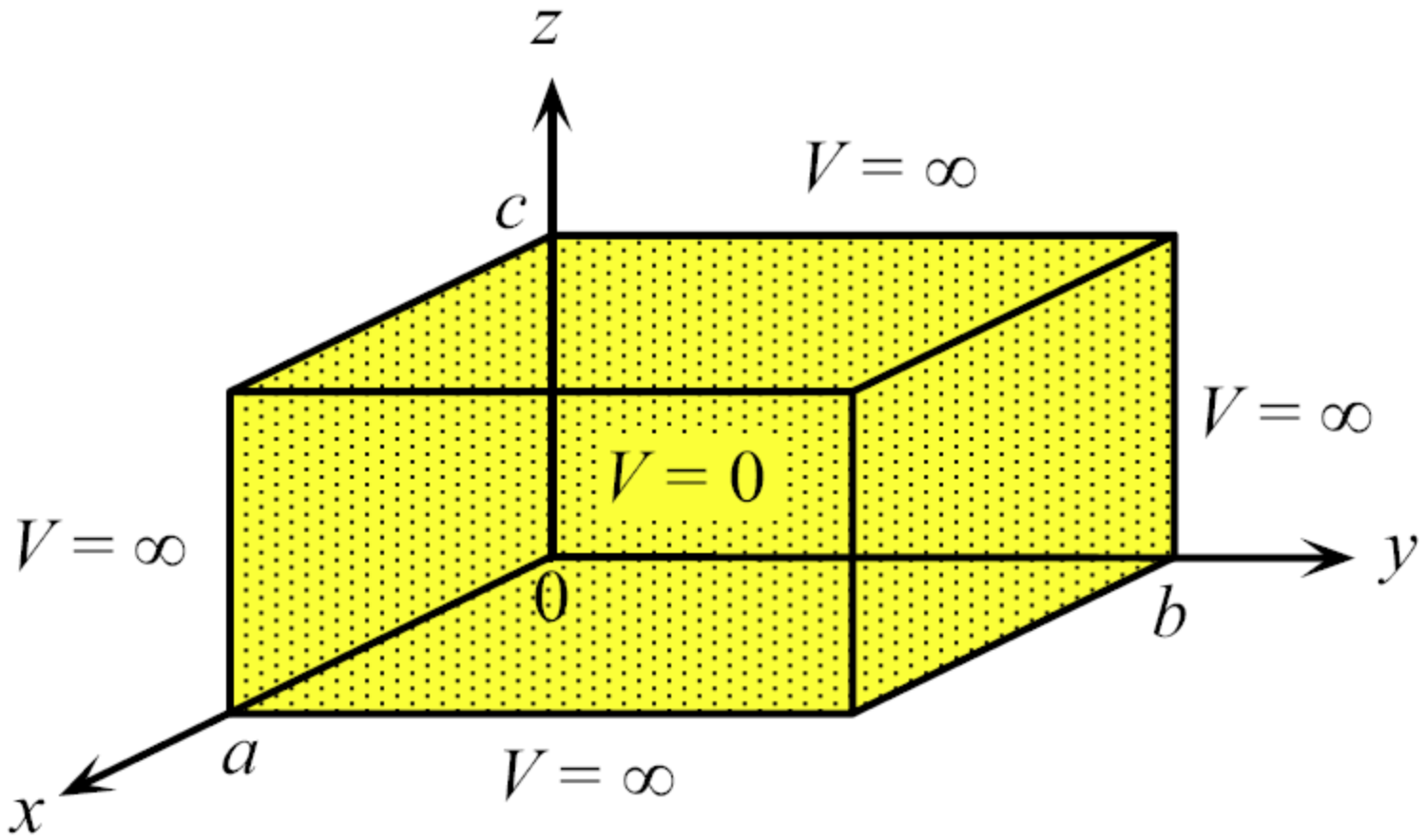

Electron confined in three dimensions by a three-dimensional infinite PE box. Everywhere inside the box, V = 0, but outside, V = ∞. The electron cannot escape from the box.

Fig 3.19

Potential Box: Three Quantum Numbers

Electron wavefunction in infinite PE well

$$\psi_{n_1 n_2 n_3}(x,y,z) = A\sin\left(\frac{n_1 \pi x}{a}\right)\sin\left(\frac{n_2 \pi y}{b}\right)\sin\left(\frac{n_3 \pi z}{c}\right)$$

Electro energy in infinite PE box

$$E_{n_1 n_2 n_3} = \frac{h^2\left(n_1^2 + n_2^2 + n_3^2\right)}{8ma^2} = \frac{h^2 N^2}{8ma^2}$$

$$N^2 = n_1^2 + n_2^2 + n_3^2$$

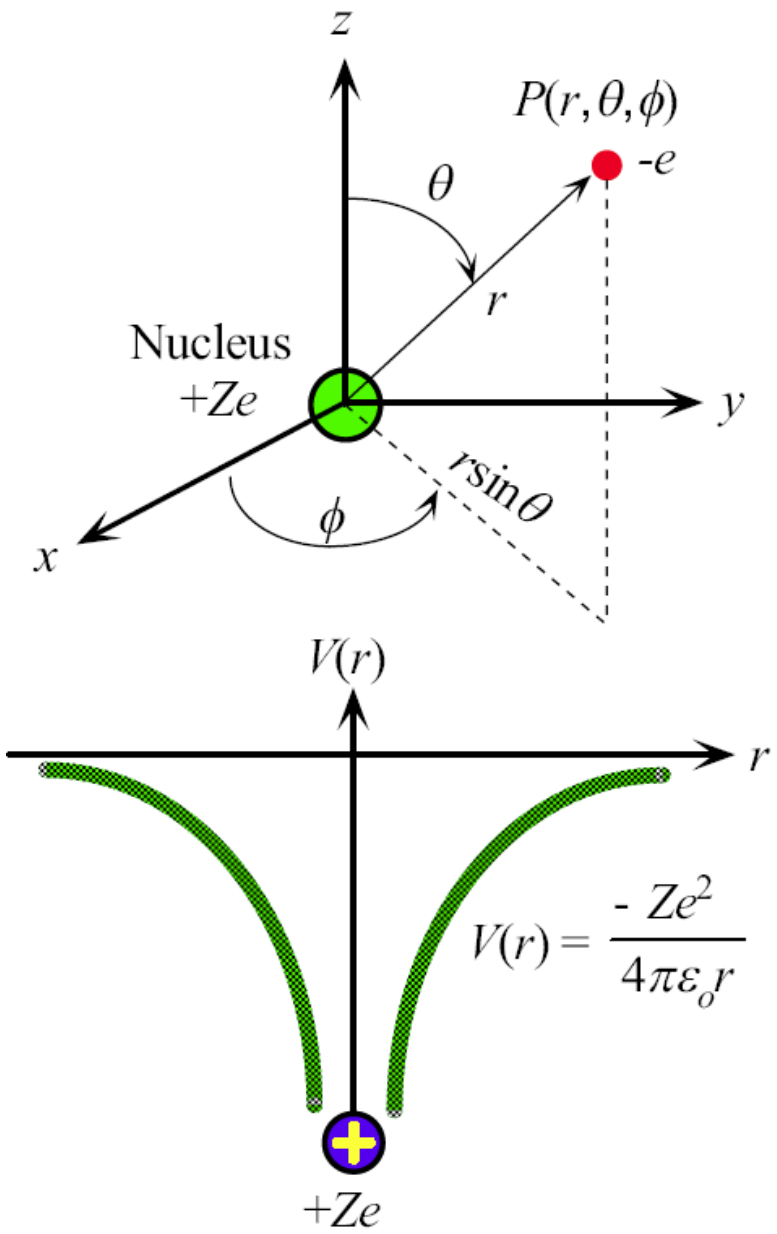

The electron in the hydrogenic atom is atom is attracted by a central force that is always directed toward the positive Nucleus.

Spherical coordinates centered at the nucleus are used to describe the position of the electron. The *PE* of the electron depends only on *r*.

Fig 3.20

Electron wavefunctions and the electron energy are obtained by solving the Schrödinger equation

Electron's PE $V(r)$ in hydrogenic atom is used in the Schrödinger equation

$$V(r) = \frac{-Ze^2}{4\pi\varepsilon_o r}$$

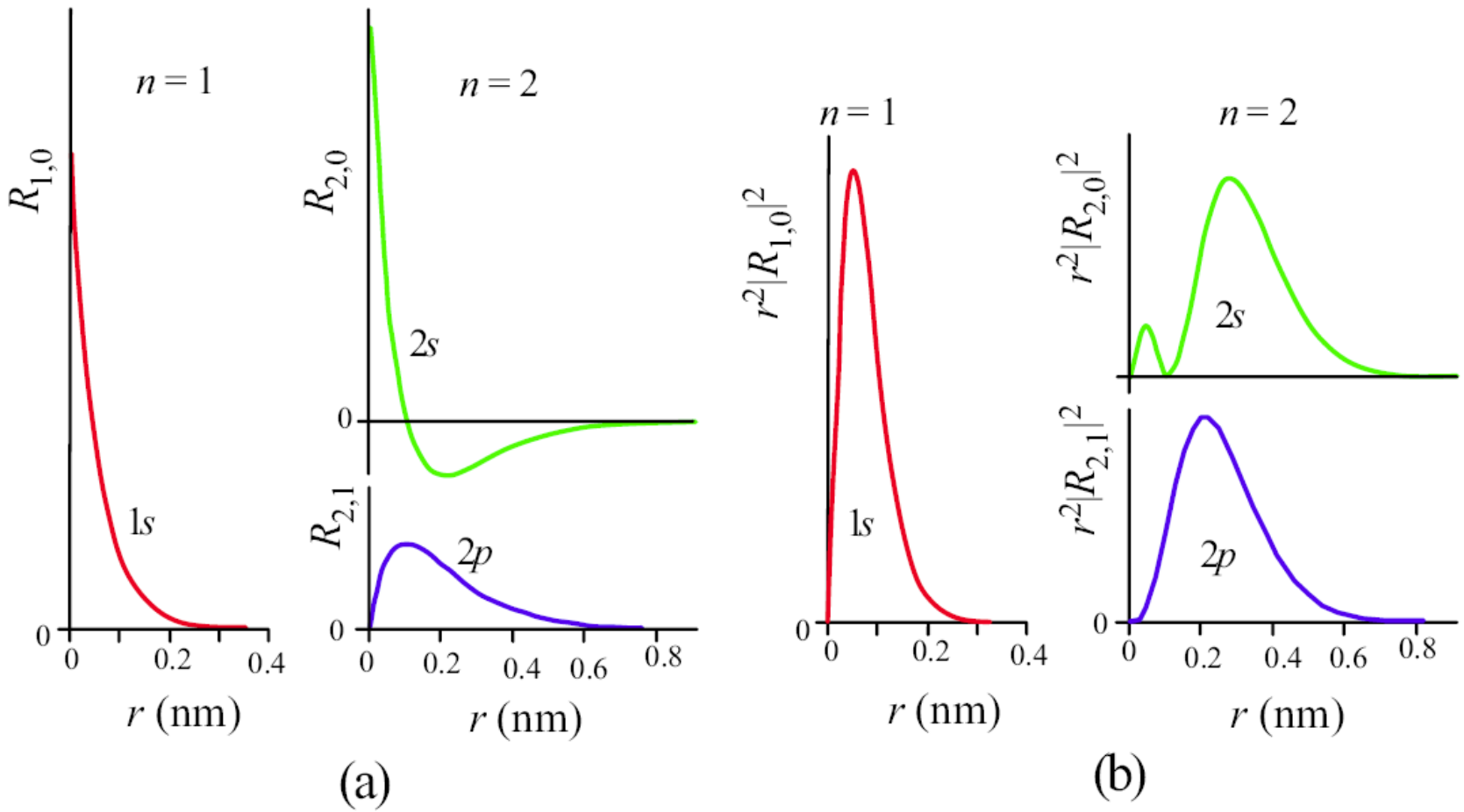

(a) Radial wavefunctions of the electron in a hydrogenic atom for various n and ℓ values. (b) $R^2\,|R_{n,\ell}{}^2|$ gives the radial probability density. Vertical axis scales are linear in arbitrary units.

Fig 3.21

Electron energy is quantized

Electron energy in the hydrogenic atom is quantized.

n is a quantum number, 1,2,3,…

$$E_n = -\frac{me^4 Z^2}{8\varepsilon_o^2 h^2 n^2}$$

Ionization energy of hydrogen: energy required to remove the electron from the ground state in the H-atom

$$E_I = \frac{me^4}{8\varepsilon_o^2 h^2} = 2.18\times10^{-18}\,\text{J} = 13.6\,\text{eV}$$

Table 3.1 Labeling of various $n\ell$ possibilities

	ℓ				
n	**0**	**1**	**2**	**3**	**4**
1	$1s$				
2	$2s$	$2p$			
3	$3s$	$3p$	$3d$		
4	$4s$	$4p$	$4d$	$4f$	
5	$5s$	$5p$	$5d$	$5f$	$5g$

Table 3.2 The radial and spherical harmonic parts of the wavefunction in the hydrogen atom ($a_o = 0.0529$ nm)

n	ℓ	$R(r)$	m_ℓ	$Y(\theta, \phi)$	
1	0	$\left(\frac{1}{a_o}\right)^{3/2} 2\exp\left(-\frac{r}{a_o}\right)$	0	$\frac{1}{2\sqrt{\pi}}$	
2	0	$\left(\frac{1}{2a_o}\right)^{3/2} \left(2-\frac{r}{a_o}\right) \exp\left(-\frac{r}{2a_o}\right)$	0	$\frac{1}{2\sqrt{\pi}}$	
2	1	$\left(\frac{1}{2a_o}\right)^{3/2} \left(\frac{r}{\sqrt{3}a_o}\right) \exp\left(-\frac{r}{2a_o}\right)$	0	$\frac{1}{2}\sqrt{\frac{3}{\pi}}\cos\theta$	$\propto \sin\theta\cos\phi$
			1	$\frac{1}{2}\sqrt{\frac{3}{2\pi}}\sin\theta e^{j\phi}$	
			−1	$\frac{1}{2}\sqrt{\frac{3}{2\pi}}\sin\theta e^{-j\phi}$	$\propto \sin\theta\sin\phi$

Correspond to $m_\ell = -1$ and $+1$.

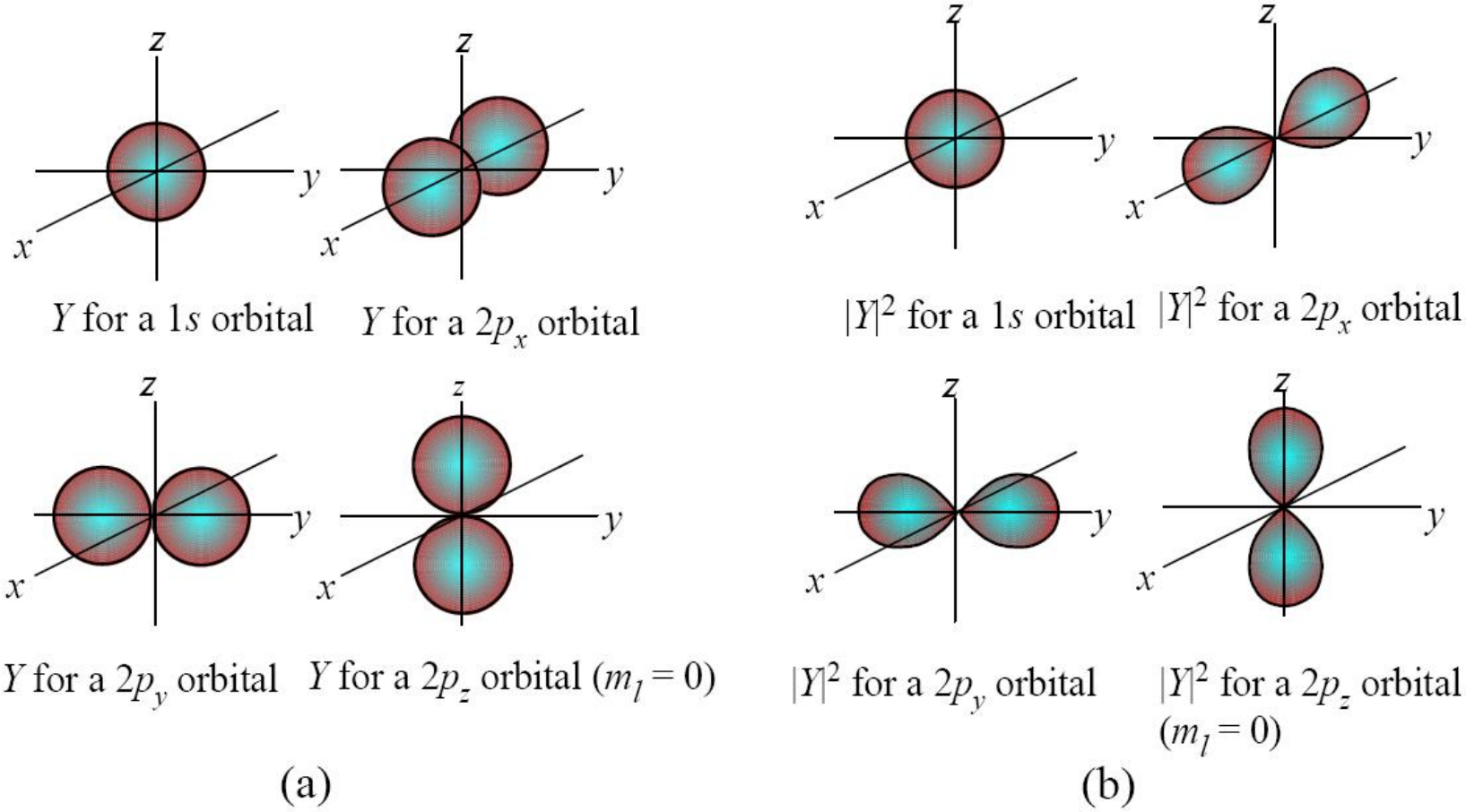

(a) The polar plots of $Y_{n,\ell}(\theta, \phi)$ for 1*s* and 2*p* states.
(b) The angular dependence of the probability distribution, which is proportional to $|Yn,\ell(\theta, \phi)|^2$.

Fig 3.22

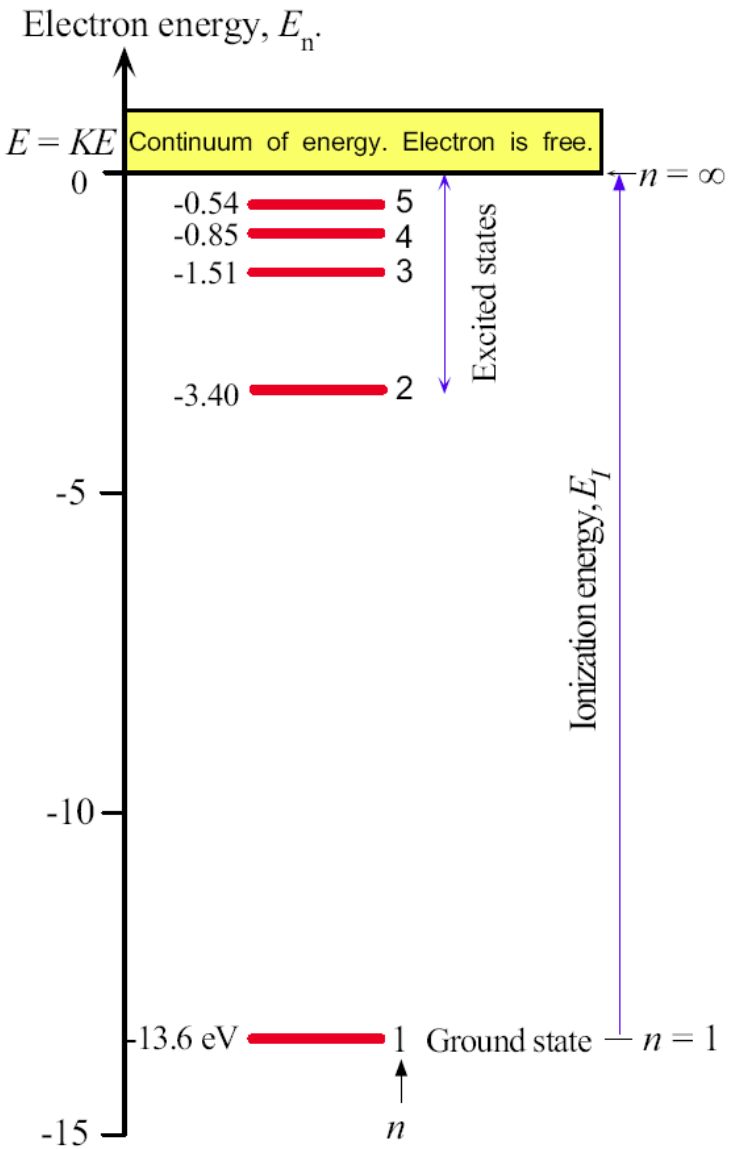

The energy of the electron in the hydrogen atom ($Z = 1$).

Fig 3.23

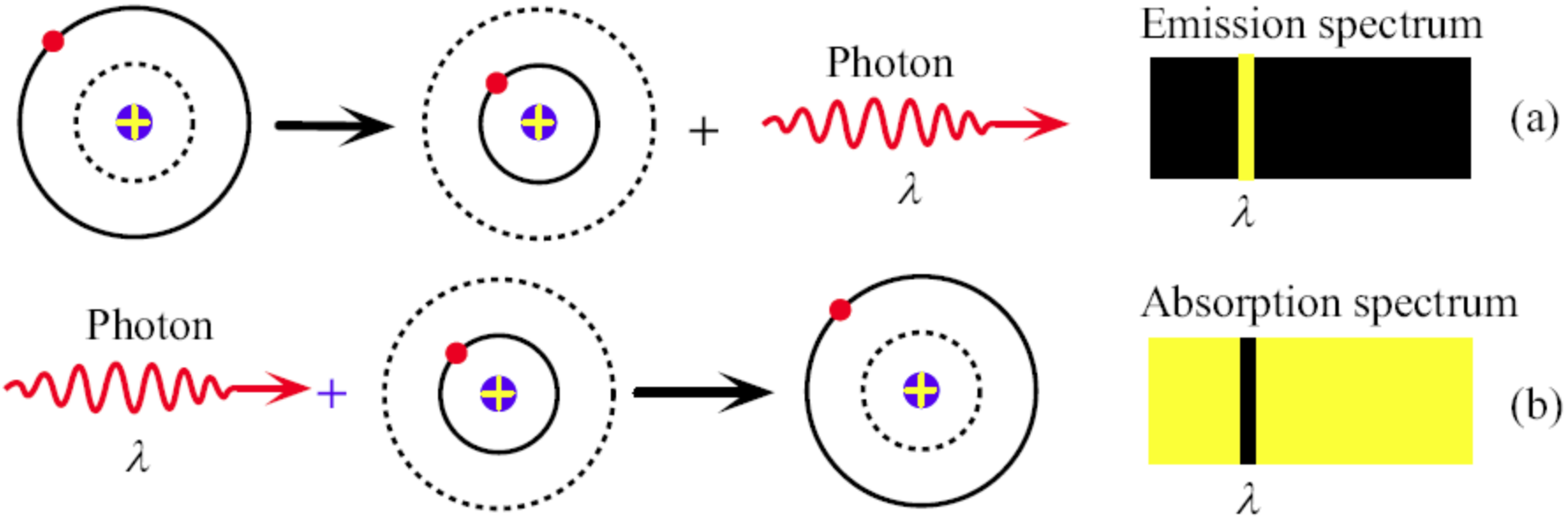

The physical origin of spectra.

(a) Emission
(b) Absorption

Fig 3.24

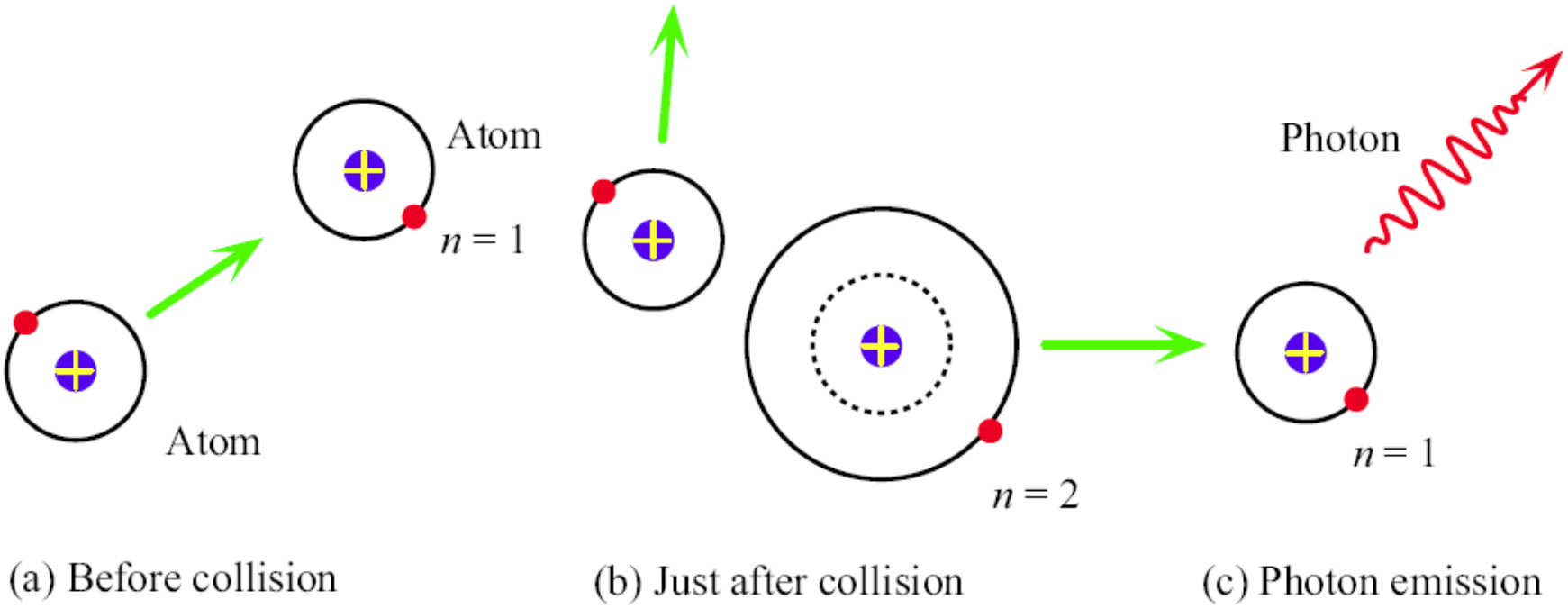

An atom can become excited by a collision with another atom.
When it returns to its ground energy state, the atom emits a photon.

Fig 3.25

Electron probability distribution in the hydrogen atom

Maximum probability for $\ell = n - 1$

$$r_{\max} = \frac{n^2 a_o}{Z}$$

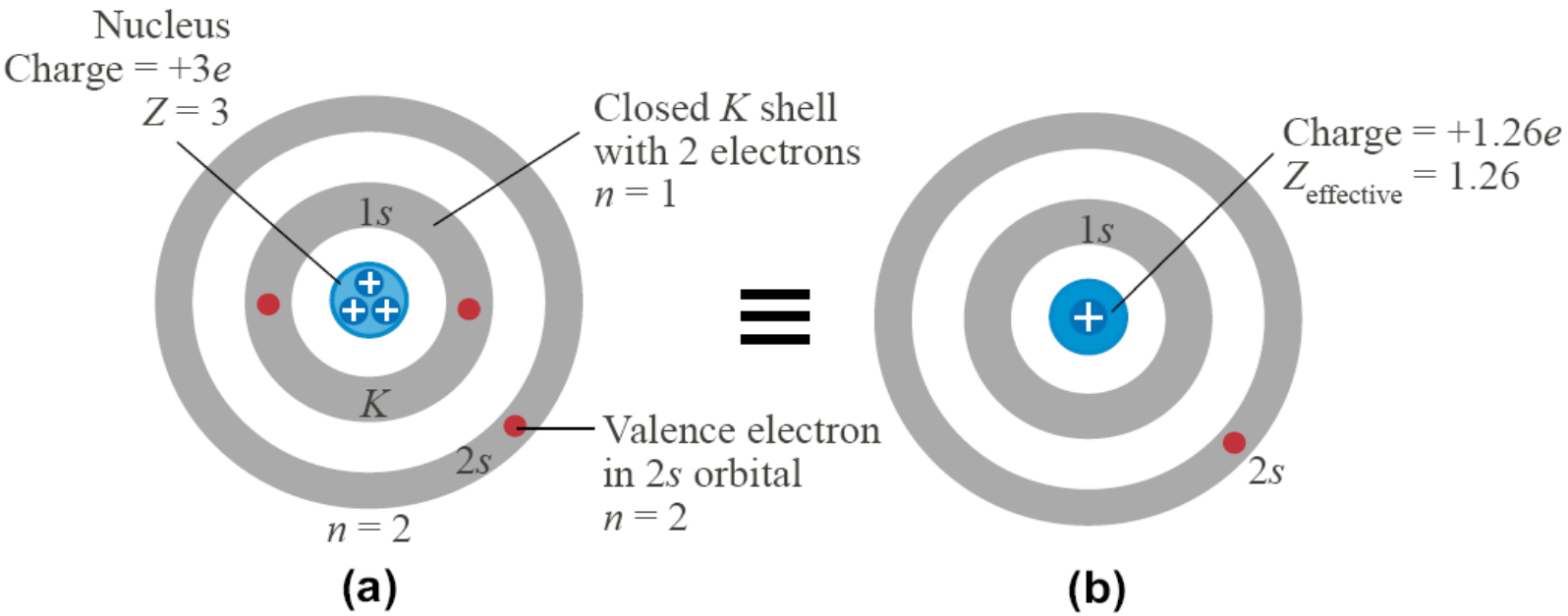

The Li atom has a nucleus with charge +3e, 2 electrons in the *K* shell , which is closed, and one electron in the 2*s* orbital. (b) A simple view of (a) would be one electron in the 2s orbital that sees a single positive charge, *Z* = 1

The simple view *Z* = 1 is not a satisfactory description for the outer electron because it has a probability distribution that penetrates the inner shell. We can instead use an effective *Z*, $Z_{effective}$ = 1.26, to calculate the energy of the outer electron in the Li atom.

Fig 3.26

Ionization energy from the *n*-level for an outer electron

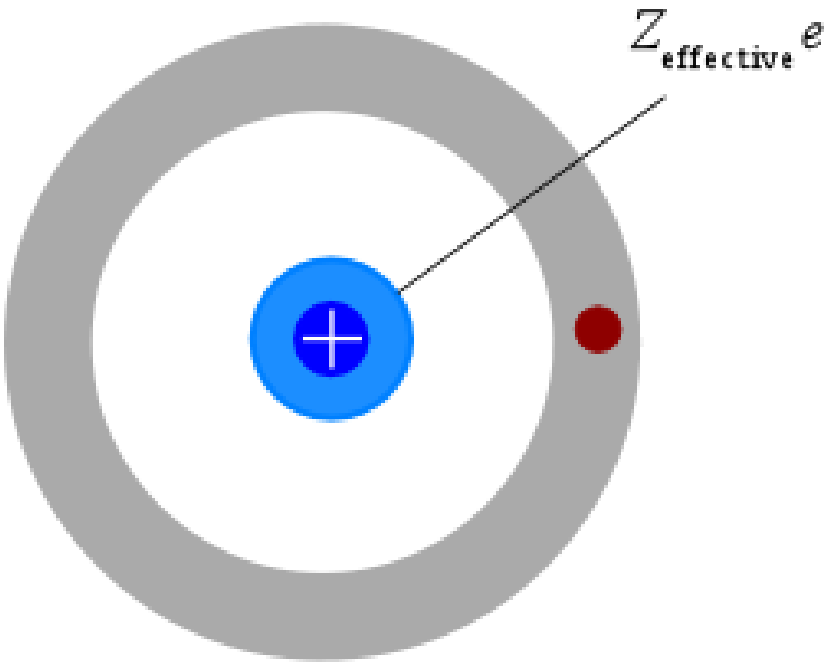

$$E_{I,n} = \frac{Z_{\text{effective}}^2\,(13.6\,\text{eV})}{n^2}$$

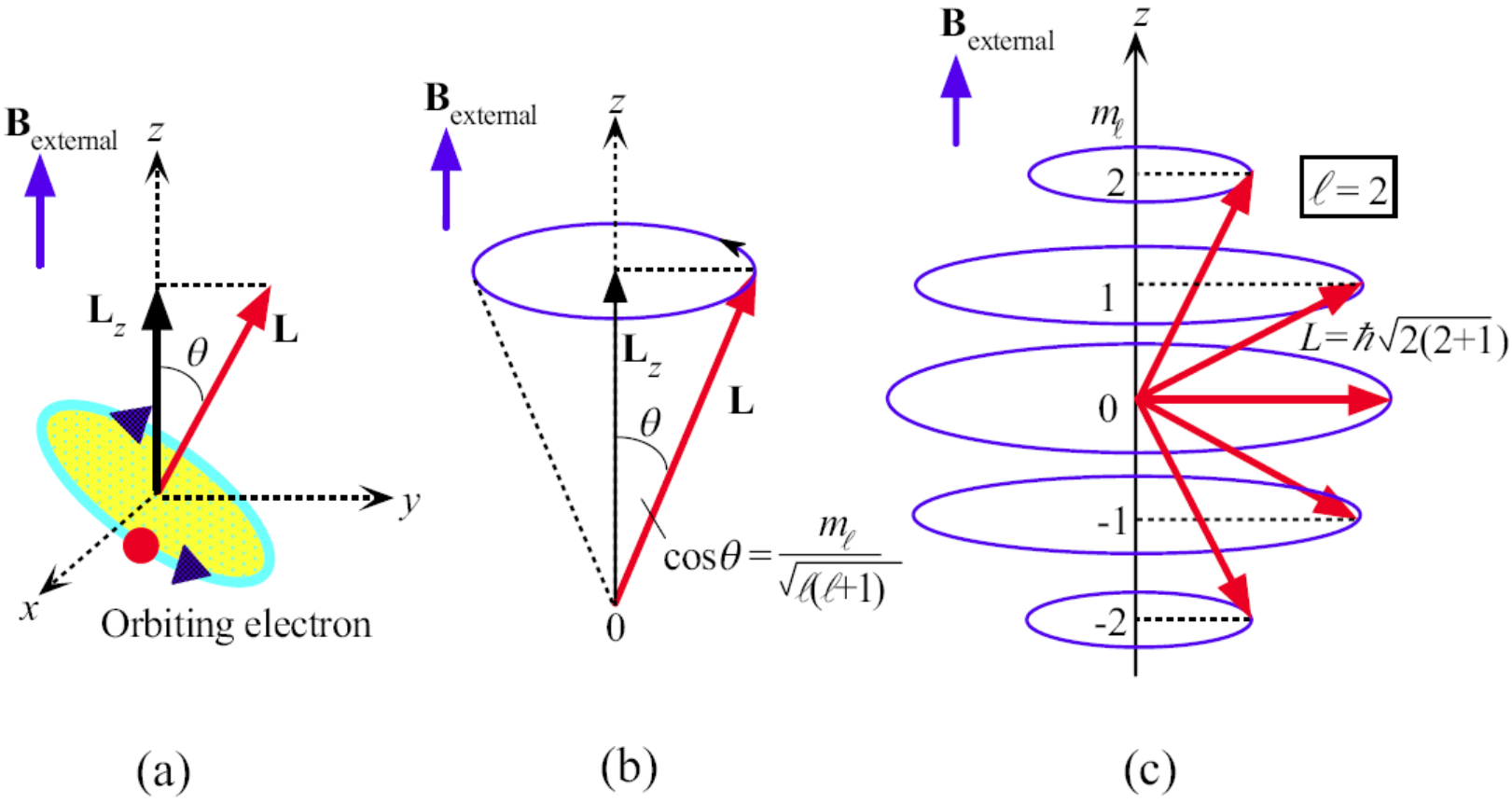

(a) The electron has an orbital angular momentum, which has a quantized component **L** along an external Magnetic field $\mathbf{B}_{external}$.
(b) The orbital angular momentum vector **L** rotates about the z axis. Its component $\mathbf{L}_z$ is quantized; Therefore, the **L** orientation, which is the angle θ, is also quantized. **L** traces out a cone.
(c) According to quantum mechanics, only certain orientations (θ) for **L** are allowed, as determined by ℓ and m_ℓ

Fig 3.27

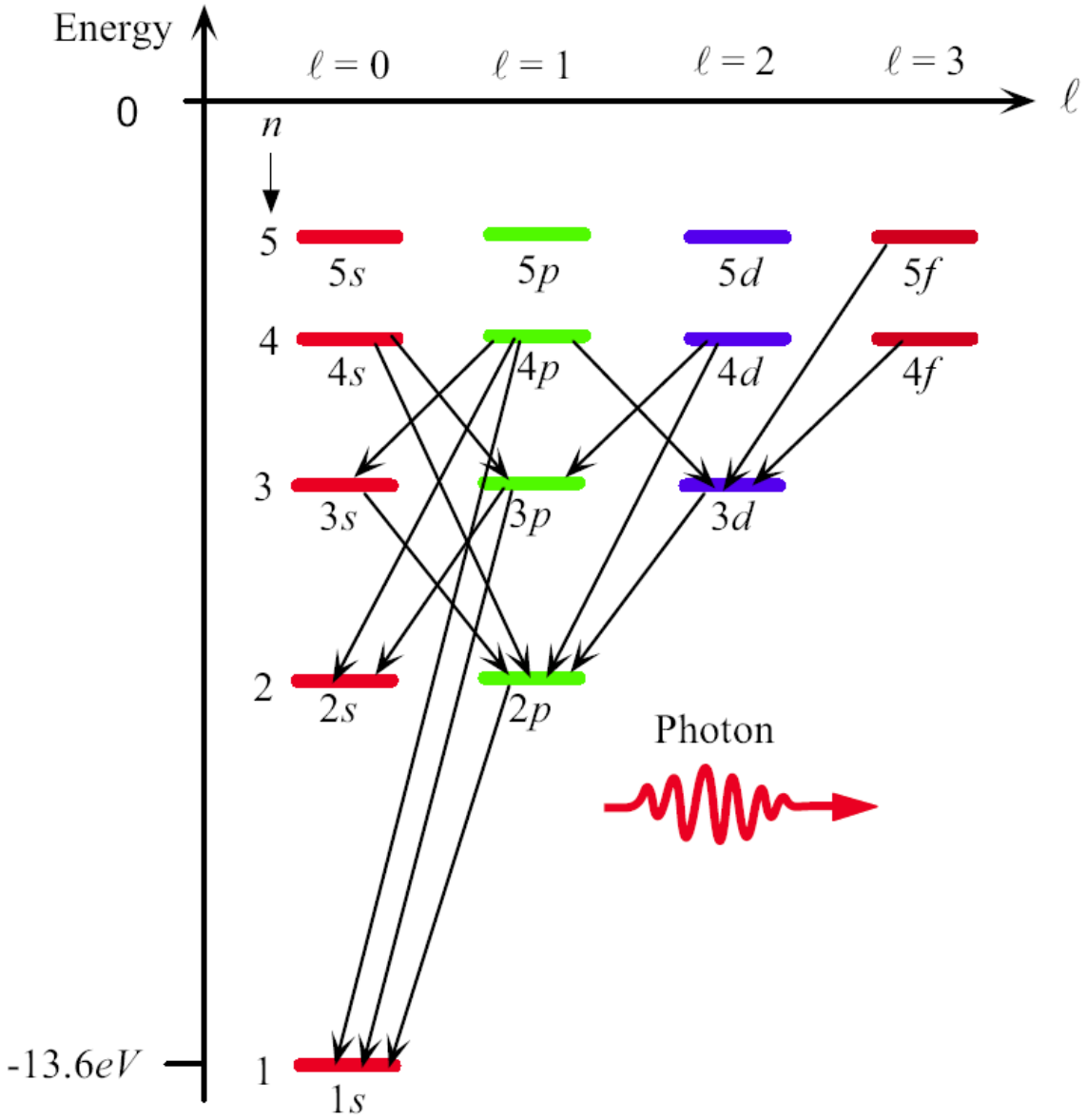

An illustration of the allowed Photon emission processes. Photon emission involves $\Delta\ell = \pm 1$,

Fig 3.28

Orbital Angular Momentum and Space Quantization

Orbital angular momentum

$$L = \hbar\left[\ell(\ell+1)\right]^{1/2}$$

where $\ell = 0, 1, 2, \ldots . n-1$

Orbital angular momentum along B_z

$$L_z = m_\ell \hbar$$

Selection rules for *EM* radiation absorption and emission

$$\Delta\ell = \pm 1 \quad \text{and} \quad \Delta m_\ell = 0, \pm 1$$

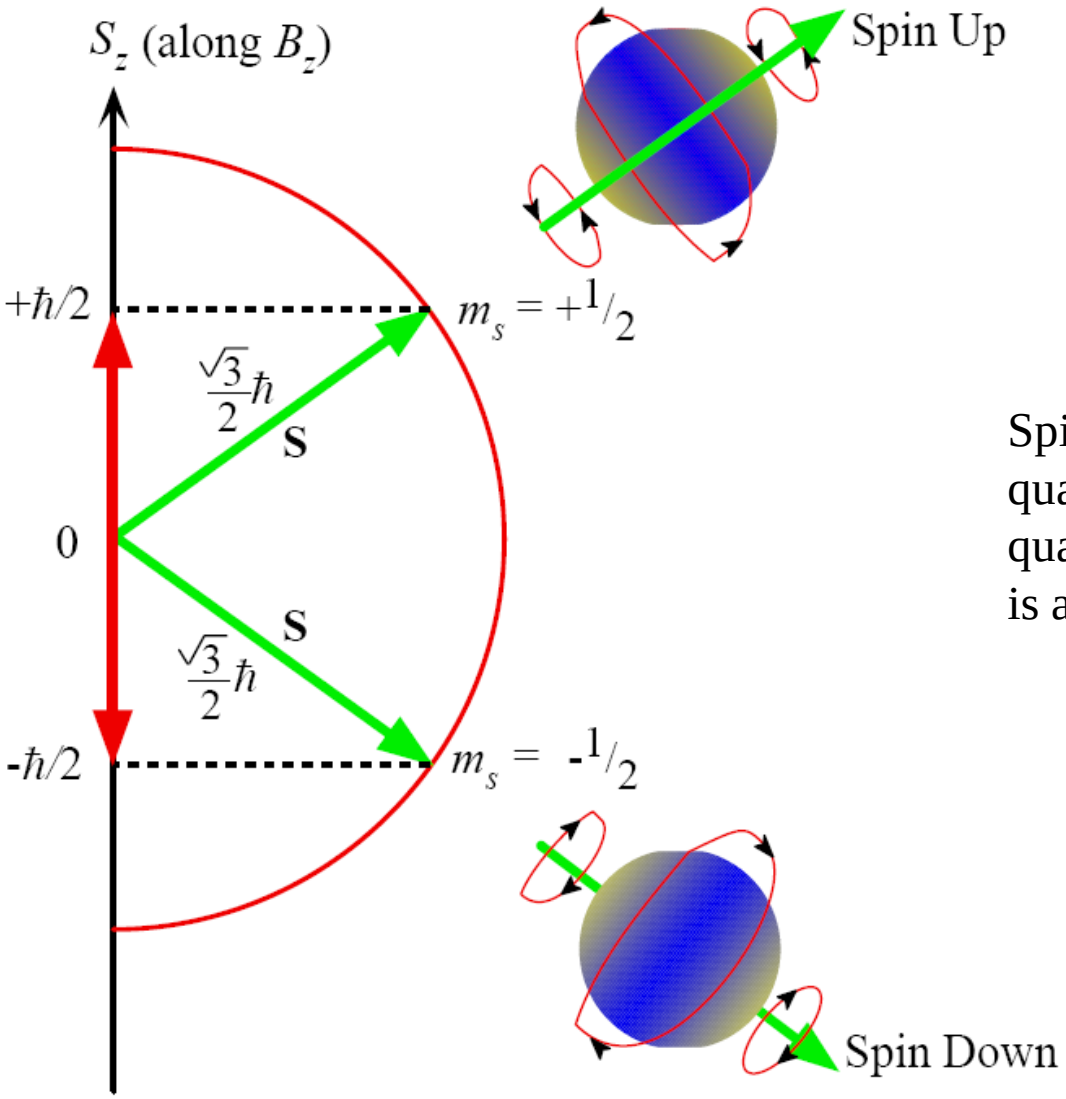

Spin angular momentum exhibits space quantization. Its magnitude along z is quantized, so the angle of S to the z axis is also quantized.

Fig 3.29

Electron Spin and Intrinsic Angular Momentum *S*

Electron spin

$$S = \hbar\left[s(s+1)\right]^{1/2} \qquad s = \frac{1}{2}$$

Spin along magnetic field

$$S_z = m_s\hbar \qquad m_s = \pm\frac{1}{2}$$

the quantum numbers s and m_s, are called the **spin and spin magnetic quantum numbers**.

Table 3.3 The four quantum numbers for the hydrogenic atom

n	Principal quantum number	$n = 1, 2, 3, \ldots$	Quantizes the electron energy
ℓ	Orbital angular momentum quantum number	$\ell = 0, 1, 2, \ldots (n-1)$	Quantizes the magnitude of orbital angular momentum L
m_ℓ	Magnetic quantum number	$m_\ell = 0, \pm 1, \pm 2, \ldots, \pm \ell$	Quantizes the orbital angular momentum component along a magnetic field B_z
m_s	Spin magnetic quantum number	$m_s = \pm \frac{1}{2}$	Quantizes the spin angular momentum component along a magnetic field B_z

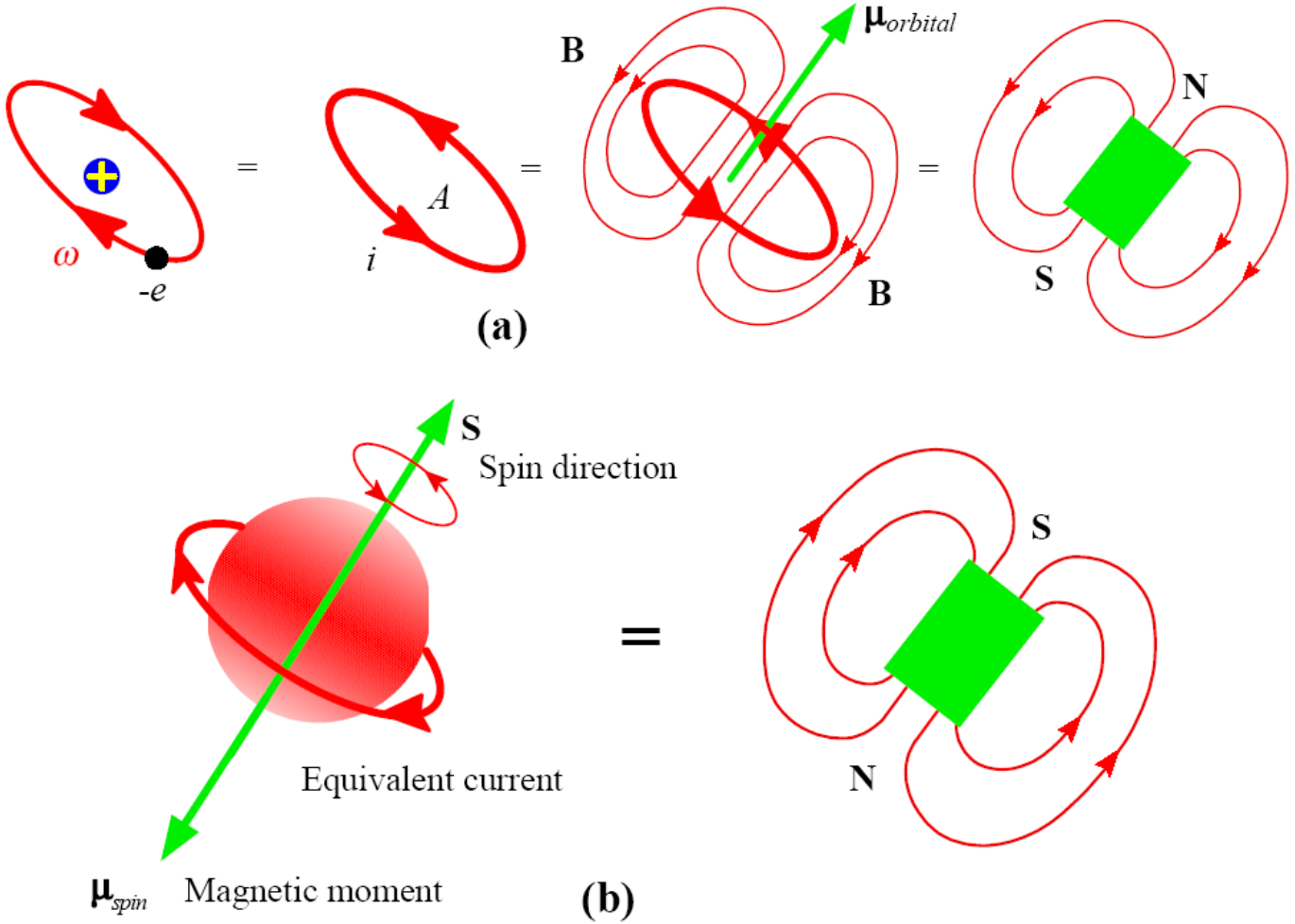

(a) The orbiting electron is equivalent to a current loop that behaves like a bar magnet.
(b) The spinning electron can be imagined to be equivalent to a current loop as shown. This current loop behaves like a bar magnet, just as in the orbital case.

Fig 3.30

Magnetic Dipole Moment of the Electron

Orbital magnetic moment

$$\boldsymbol{\mu}_{\text{orbital}} = -\frac{e}{2m_e}\mathbf{L}$$

Spin magnetic moment

$$\boldsymbol{\mu}_{\text{spin}} = -\frac{e}{m_s}\mathbf{S}$$

Energy of the electron due to its magnetic moment interacting with a magnetic field

Potential energy of a magnetic moment

$$E_{BL} = -\mu_{\text{orbital}} B \cos\theta$$

where θ is the angle between μ_{orbital} and B.

- **A magnetic moment in a magnetic field experiences a torque that tries to rotate the magnetic moment to align the moment with the field.**

- **A magnetic moment in a nonuniform magnetic field experiences force that depends on the orientation of the dipole.**

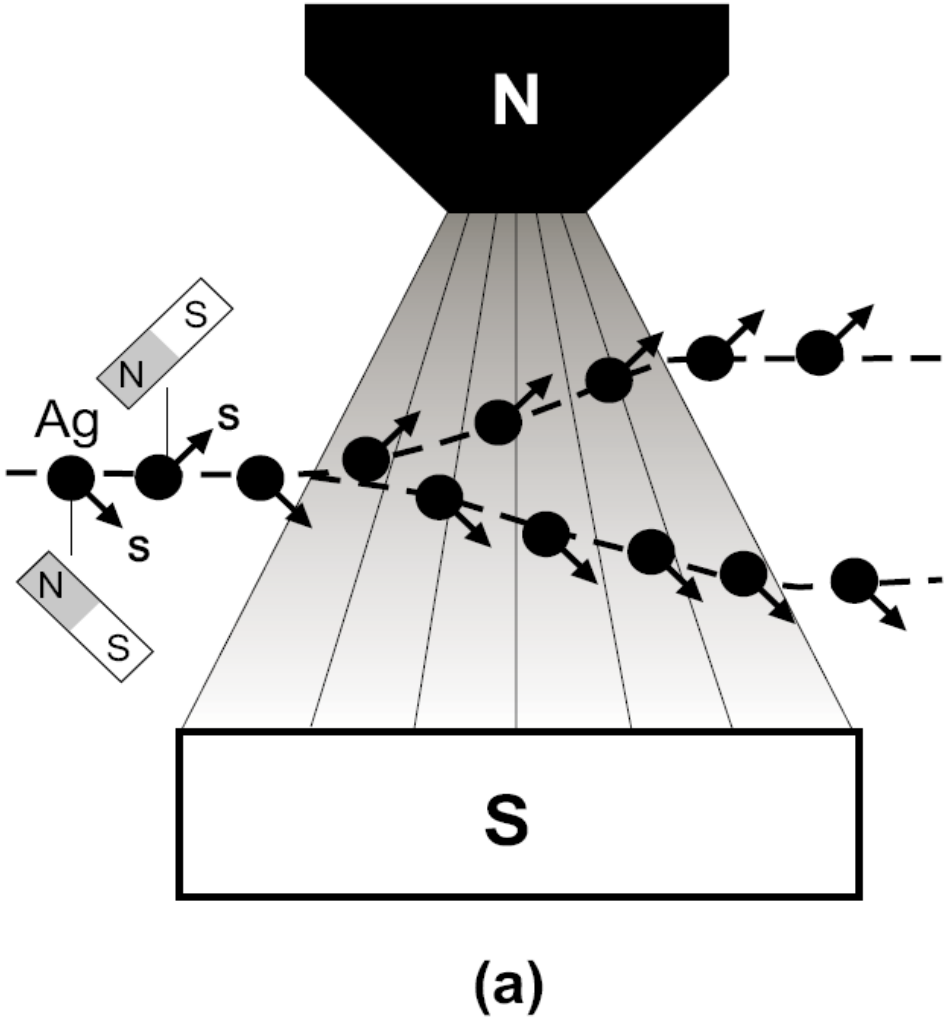

(a) Schematic illustration of the Stern-Gerlach experiment.
A stream of Ag atoms passing through a nonuniform magnetic field splits into two.

Fig 3.31

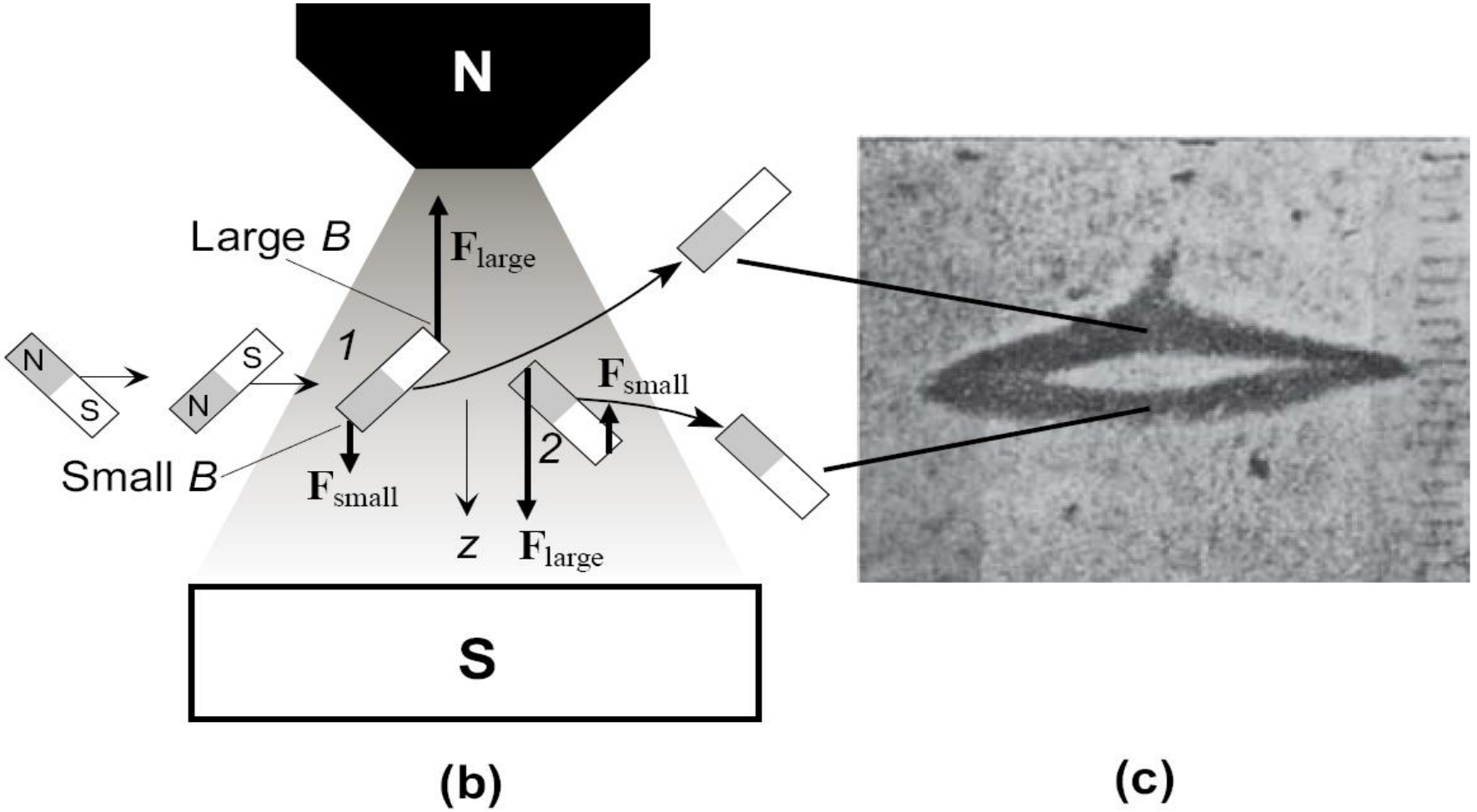

(b) Explanation of the Stern-Gerlach experiment. **(c)** Actual experimental result recorded on a photographic plate by Stern and Gerlach (O. Stern and W. Gerlach, *Zeitschr. fur. Physik*, **9**, 349, 1922.) When the field is turned off, there is only a single line on the photographic plate. Their experiment is somewhat different than the simple sketches in (a) and (b) as shown in (d).

Fig 3.31

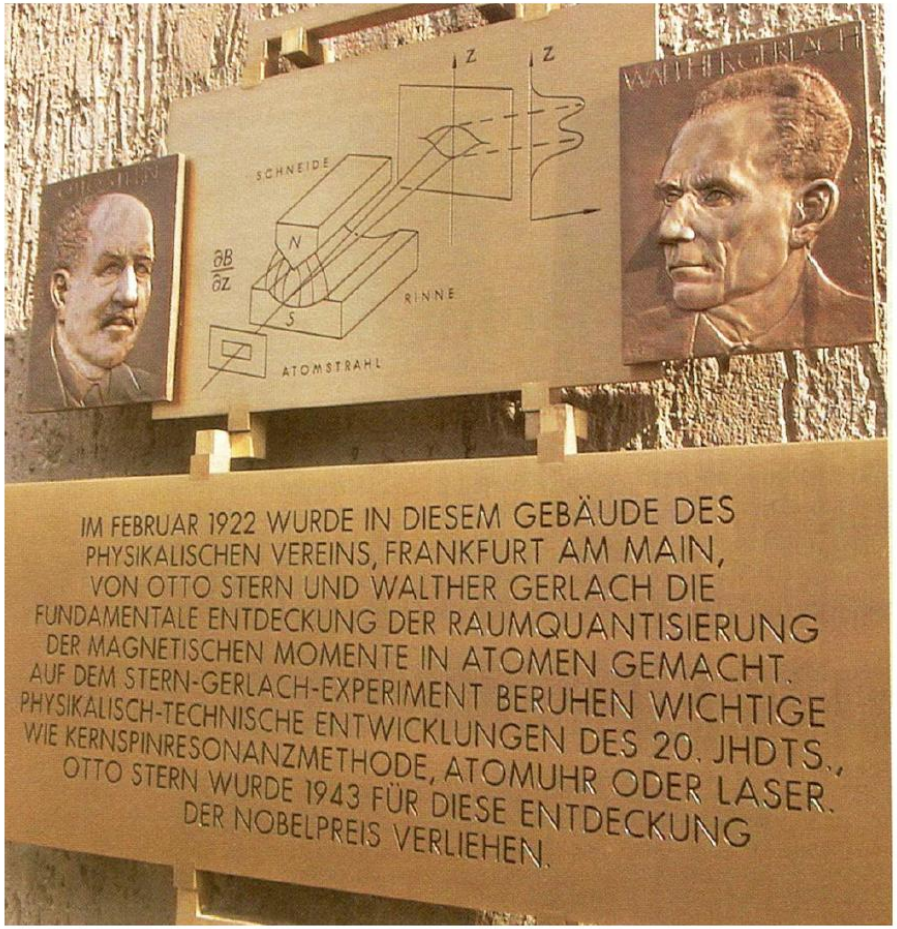

Stern-Gerlach memorial plaque at the University of Frankfurt. The drawing shows the original Stern-Gerlach experiment in which the Ag atom beam is passed along the long- length of the external magnet to increase the time spent in the nonuniform field, and hence increase the splitting. The photo on the lower right is Otto Stern (1888-1969), standing and enjoying a cigar while carrying out an experiment. Otto Stern won the Nobel prize in 1943 for development of the molecular beam technique. Plaque photo courtesy of Horst Schmidt-Böcking from B. Friedrich and D. Herschbach, "Stern and Gerlach: How a Bad Cigar Helped Reorient Atomic Physics", *Physics Today*, December 2003, p.53-59.

Fig 3.31

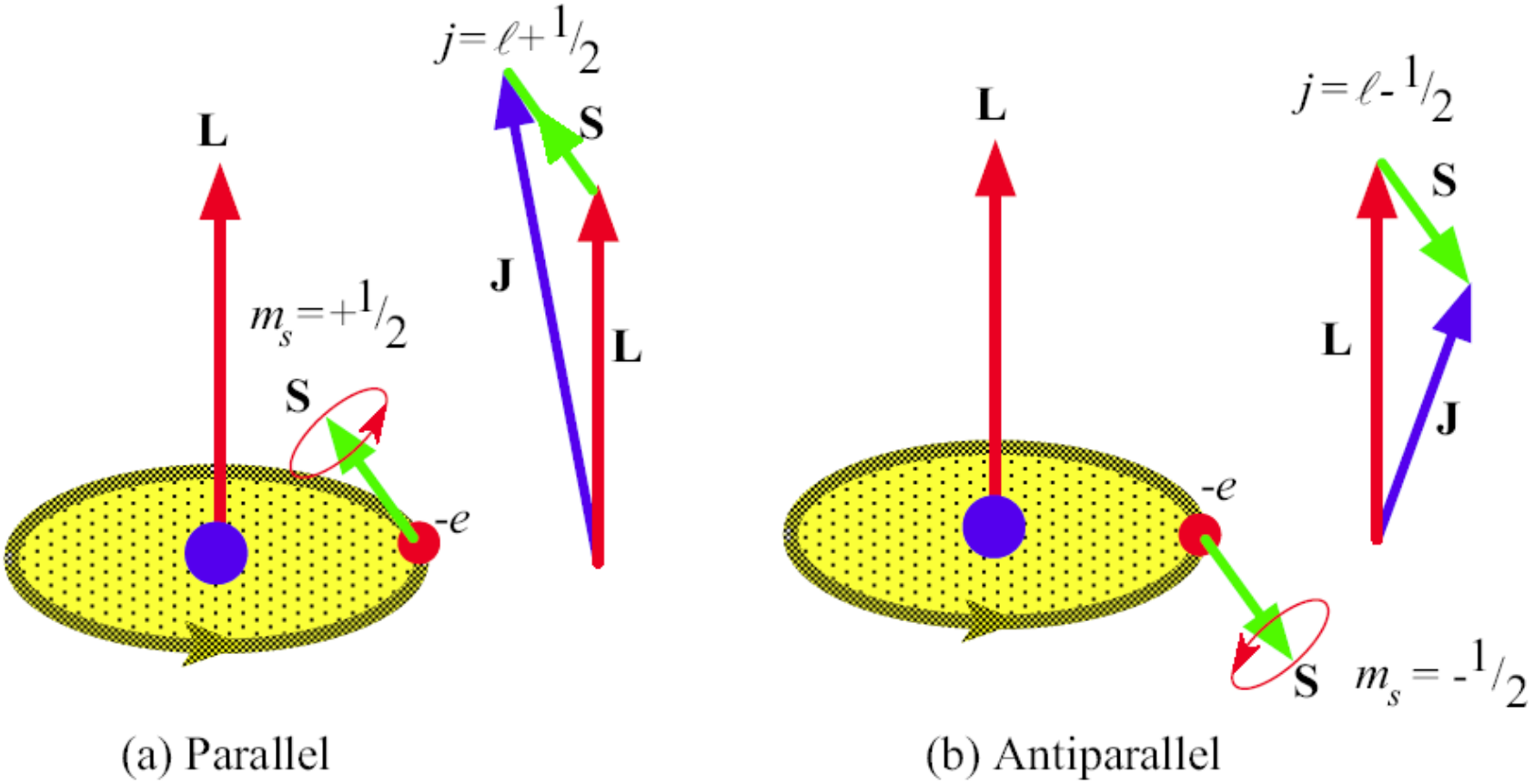

Orbital angular momentum vector **L** and spin angular momentum vector **S** can add either In parallel as in (a) or antiparallel, as in (b).
The total angular momentum vector **J** = **L** + **S**, has a magnitude J = √[j(j+1)], where in (a) j = ℓ + ½ and in (b) j = ℓ - ½

Fig 3.32

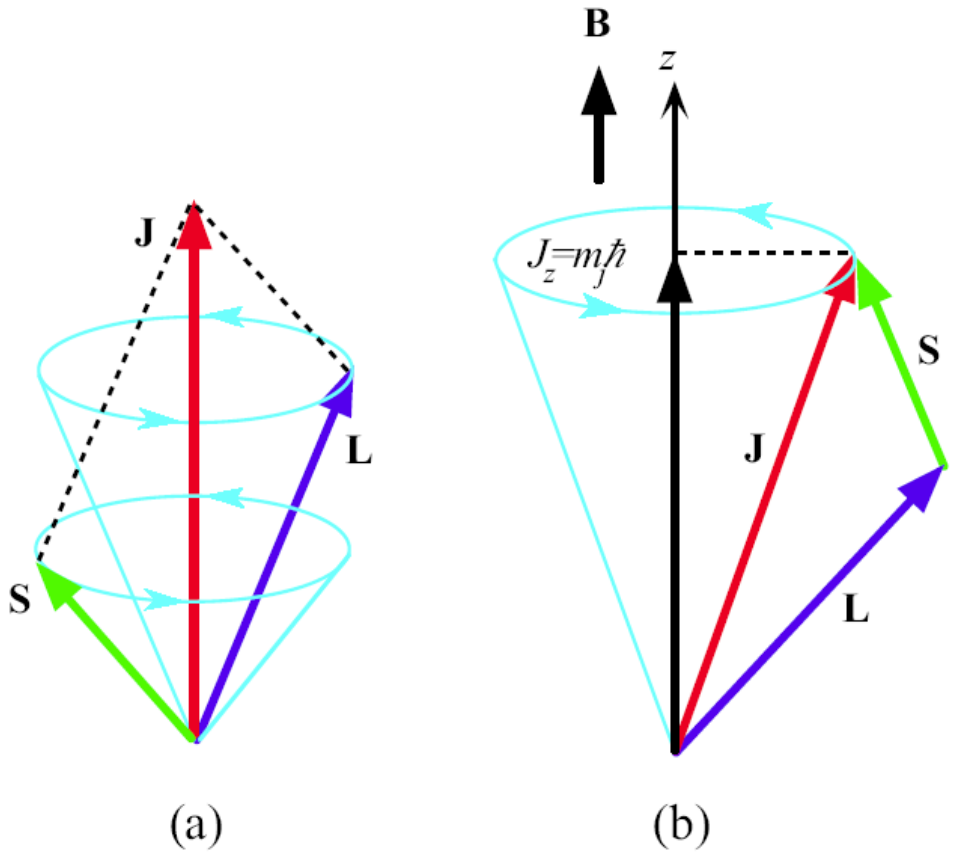

(a) The angular momentum vectors **L** and **S** precess around their resultant total angular Momentum vector **J**.
(b) The total angular momentum vector is space quantized. Vector **J** precesses about the z axis, along which its component must be $m_j\hbar$

Fig 3.33

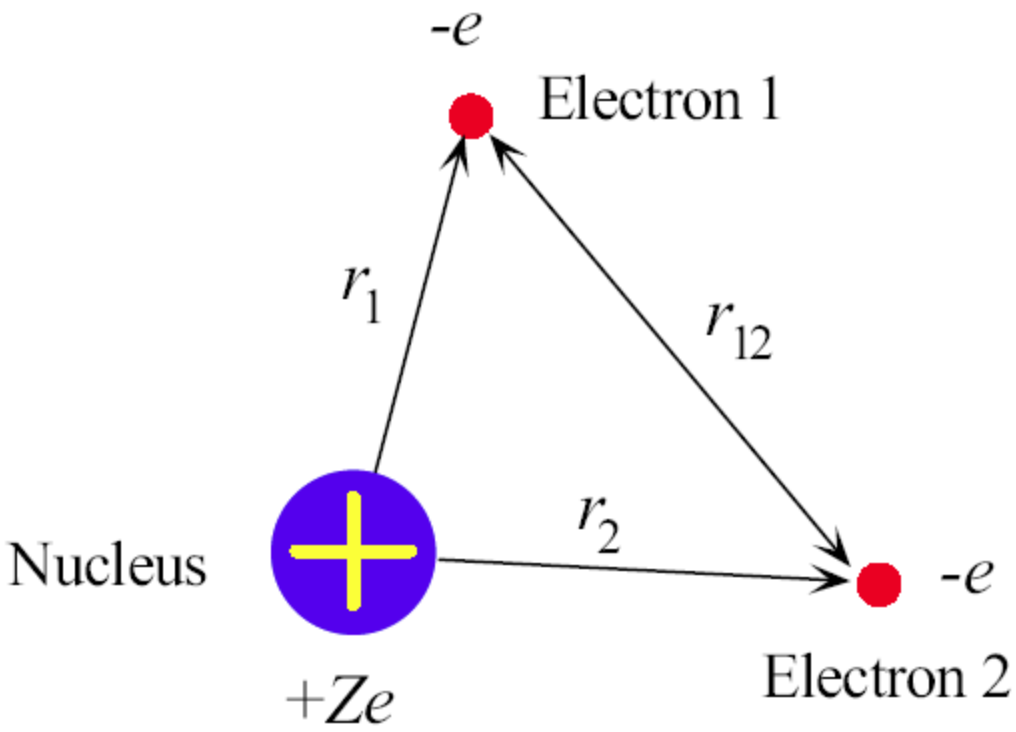

A helium-like atom
The nucleus has a charge +Ze, where Z = 2 for He. If one electron is removed, we have the He^+ ion, which is equivalent to the hydrogenic atom with Z = 2.

Fig 3.34

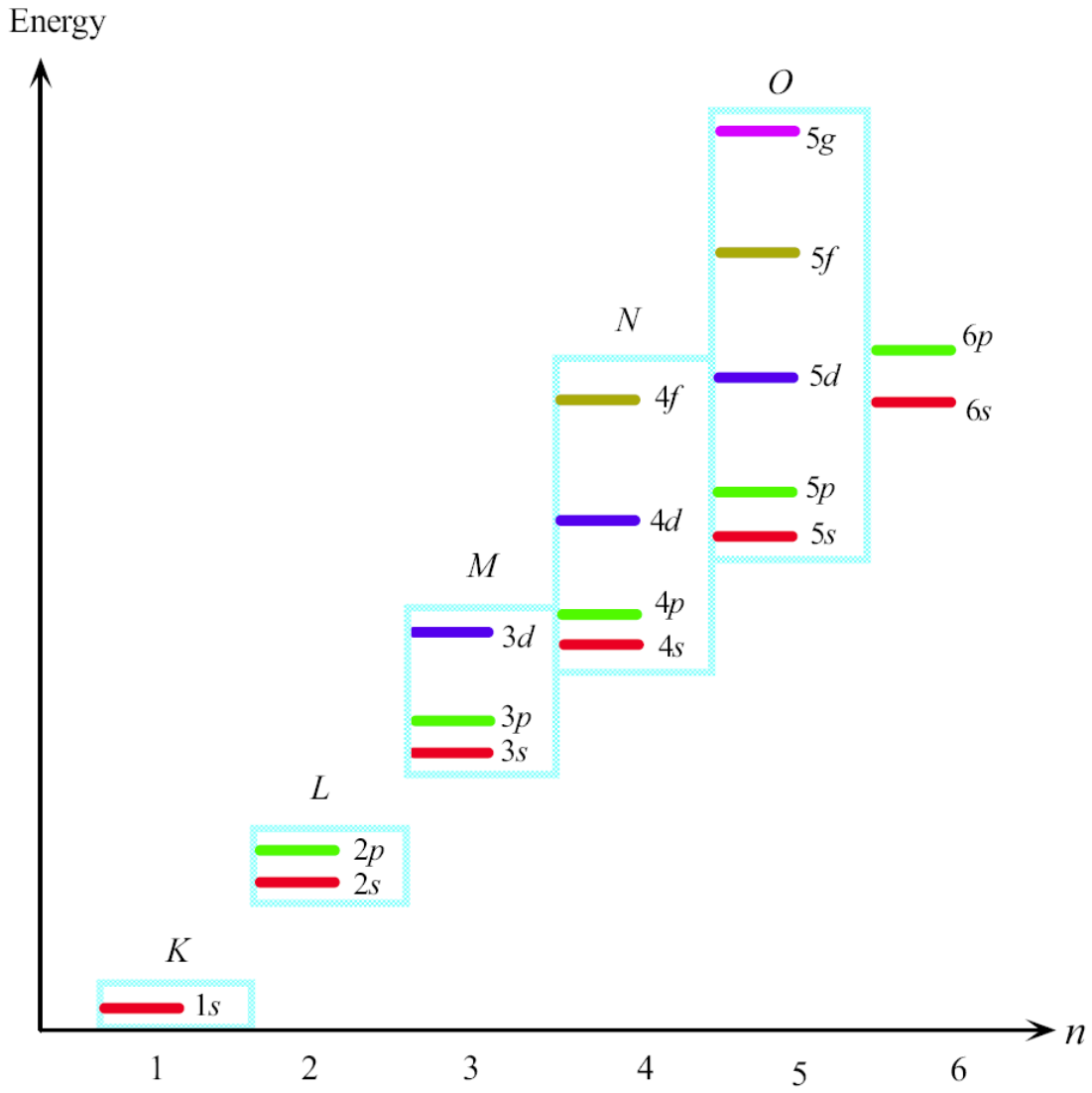

Energy of various one-electron states.
The energy depends on both n and ℓ

Fig 3.35

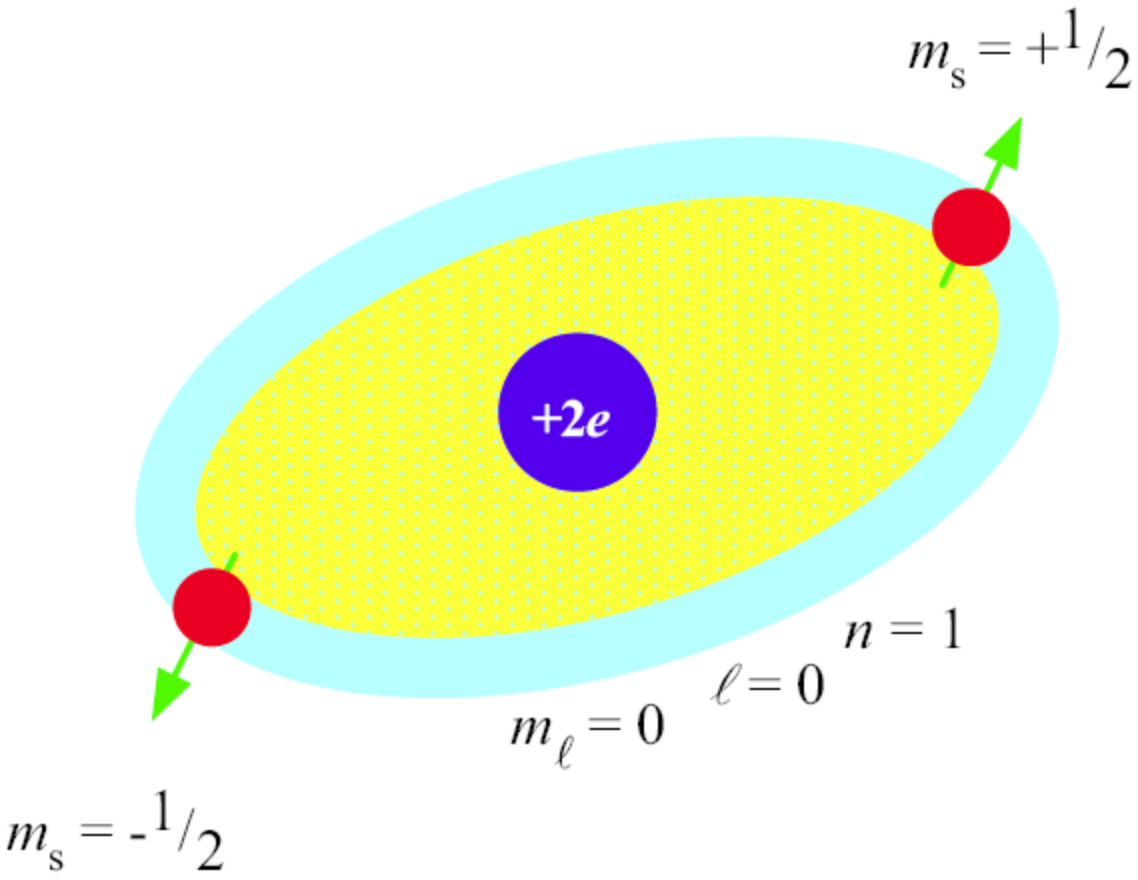

Paired spins in an orbital.

Fig 3.36

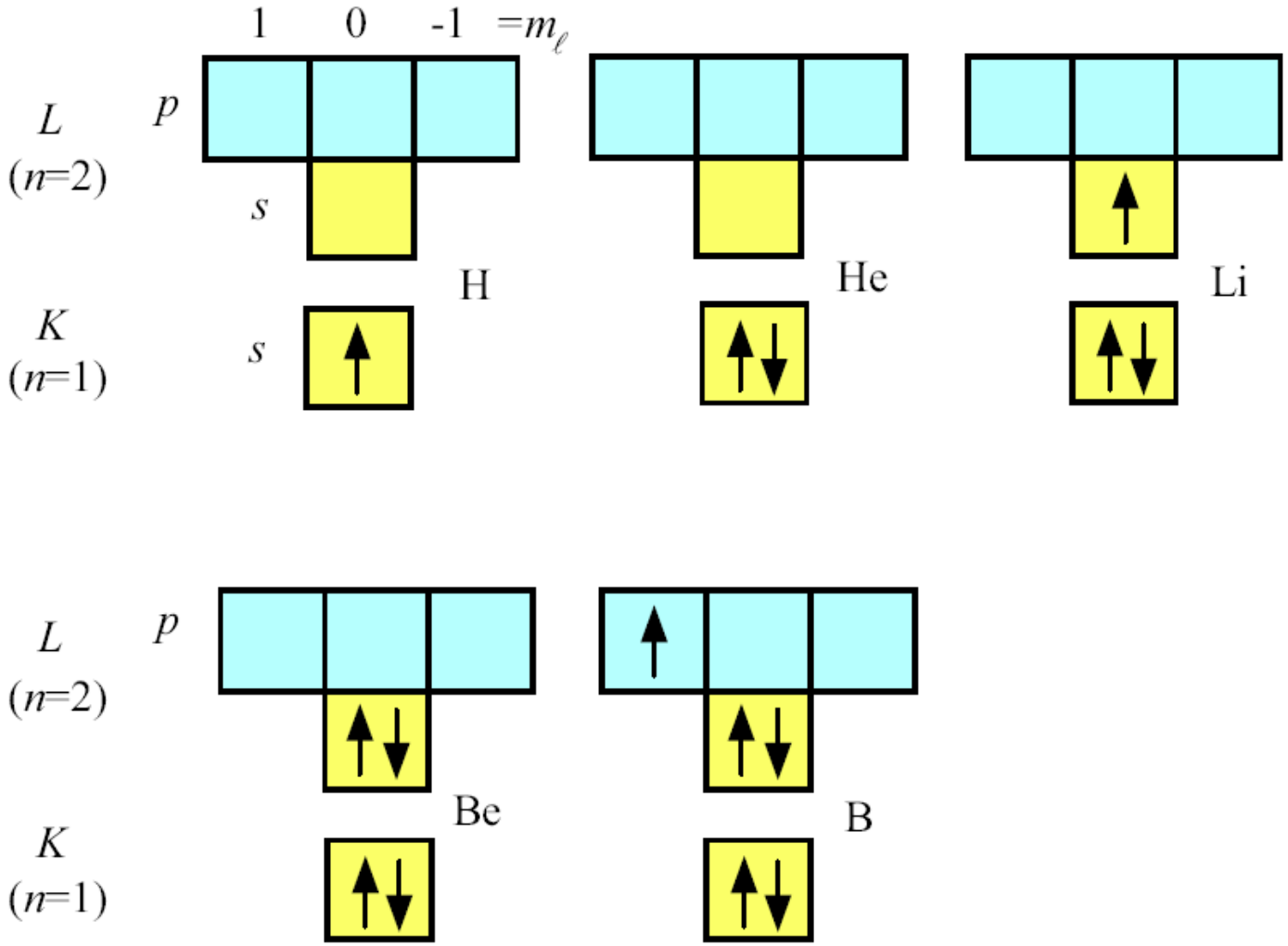

Electronic configurations for the first five elements. Each box represents an orbital $\psi\,(n, \ell, m_\ell)$

Fig 3.37

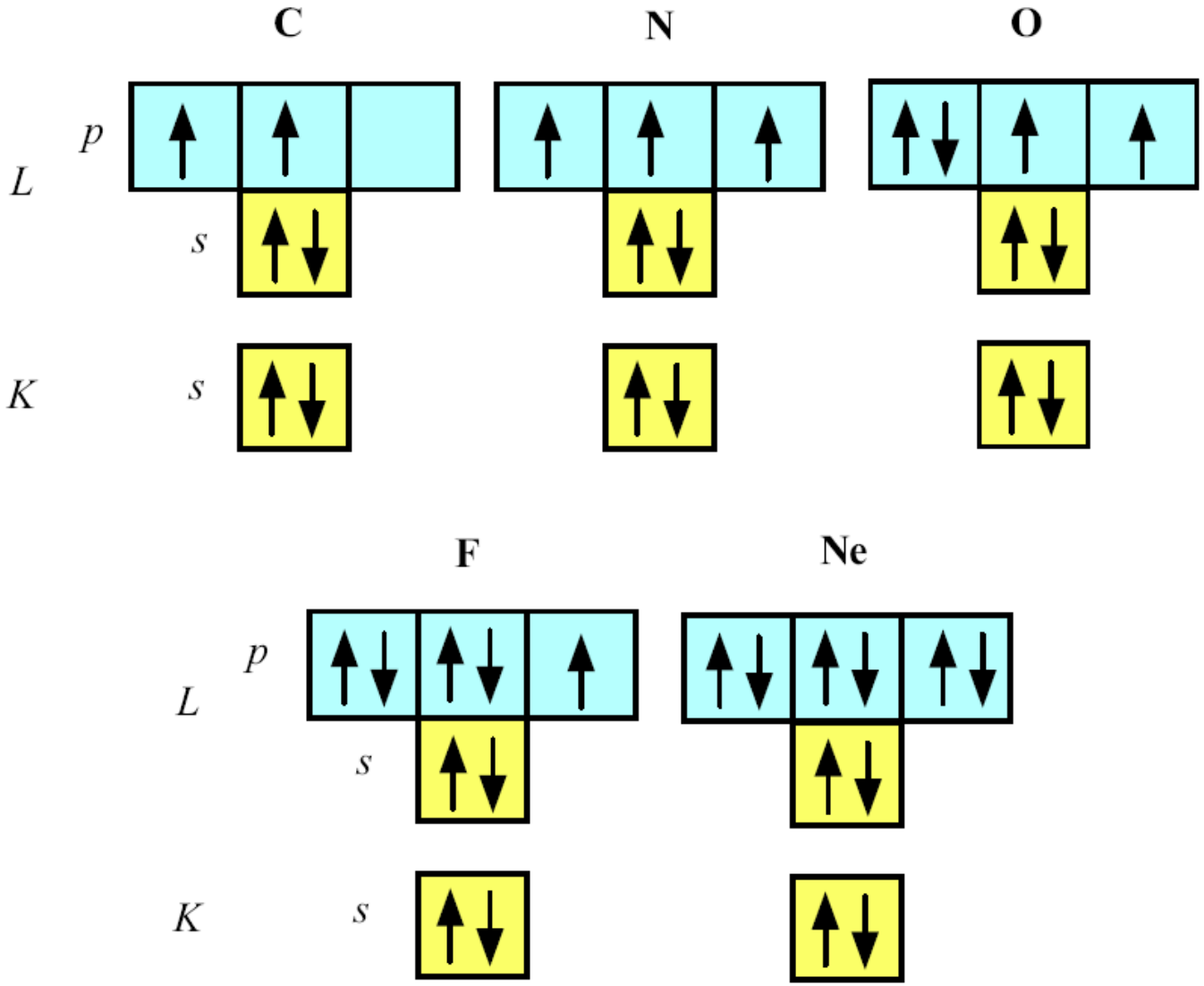

Electronic configuration for C, N, O, F and Ne atoms.
Notice that in C, N, and O, Hund's rule forces electrons to align their spins. For the Ne atom, all the K and L orbitals are full.

Fig 3.38

The Helium Atom

PE of one electron in the He atom

$$V(r_1, r_{12}) = -\frac{2e^2}{4\pi\varepsilon_o r_1} + \frac{e^2}{4\pi\varepsilon_o r_{12}}$$

Absorption, spontaneous emission and stimulated emission

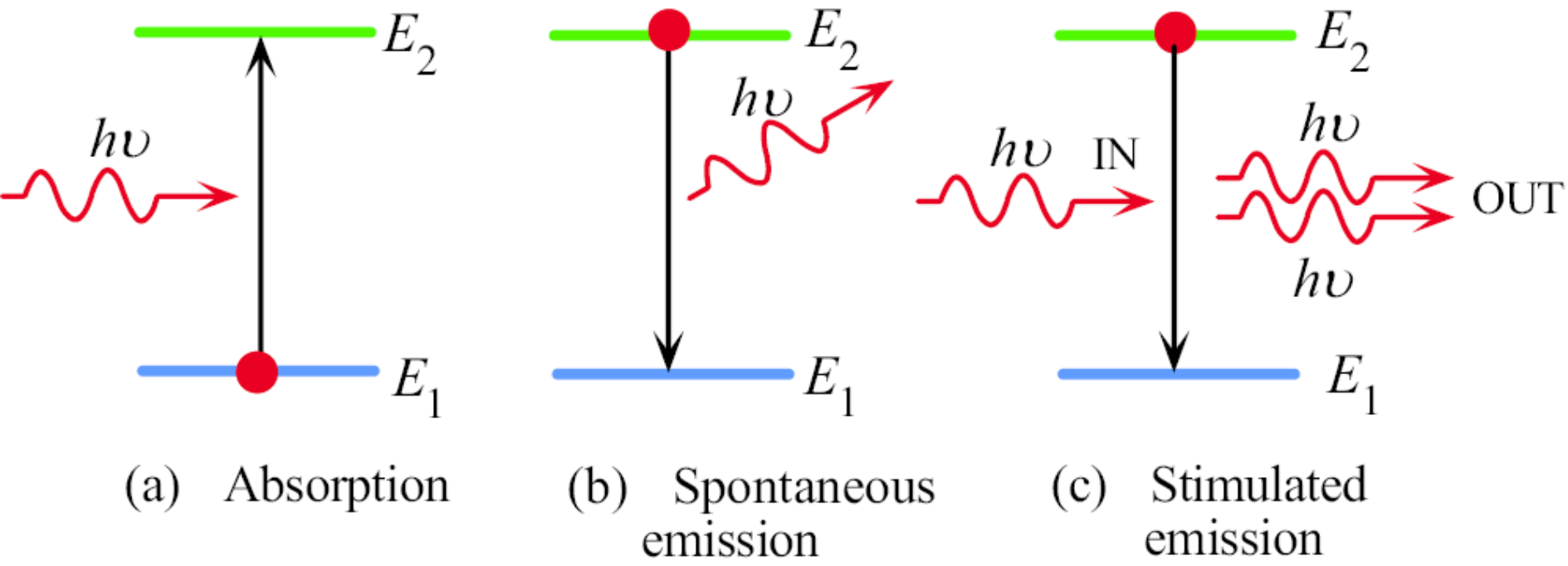

Absorption, spontaneous emission, and stimulated emission.

Fig 3.39

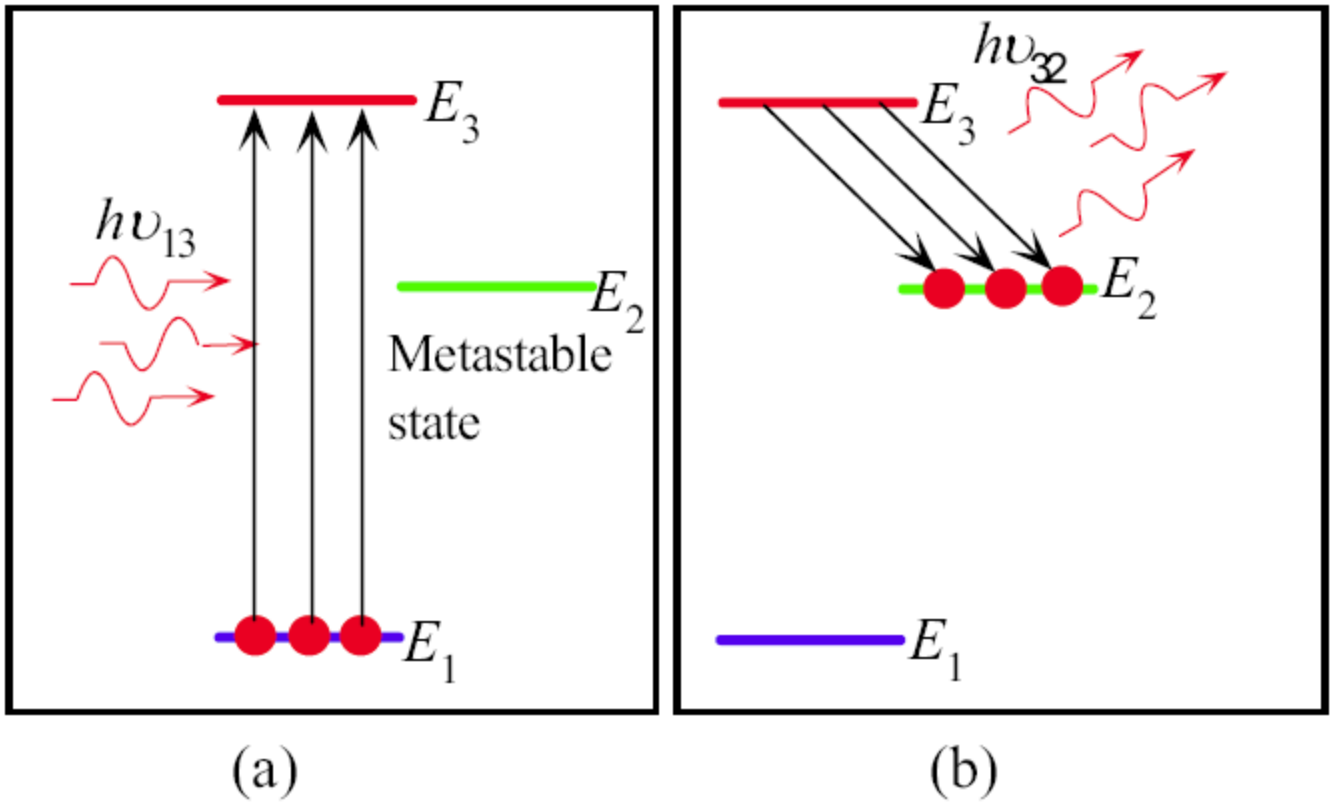

The principle of the LASER. (a) Atoms in the ground state are pumped up to the energy level E_3 by incoming photons of energy $h\upsilon_{13} = E_3-E_1$. (b) Atoms at E_3 rapidly decay to the metastable state at energy level E_2 by emitting photons or emitting lattice vibrations. $h\upsilon_{32} = E_3-E_2$.

Fig 3.40

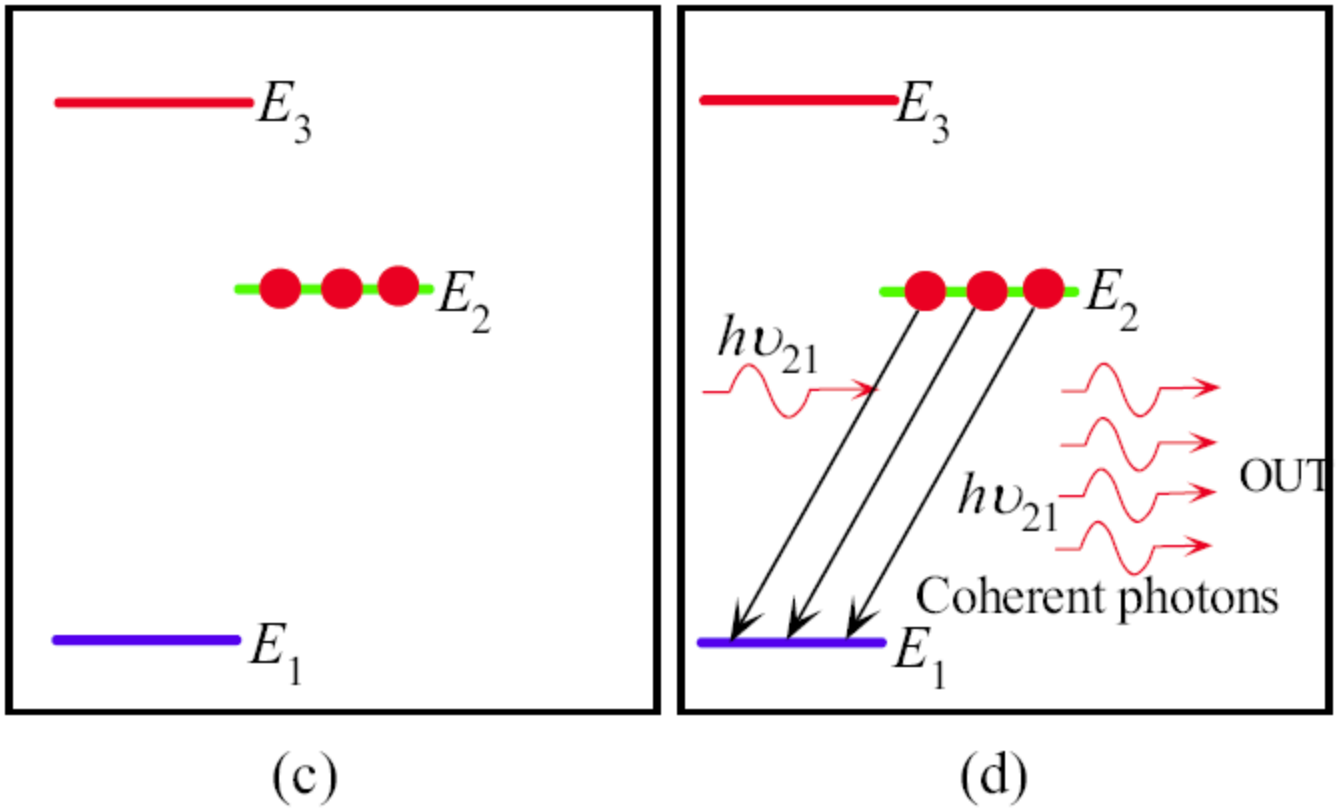

(c) As the states at E_2 are metastable, they quickly become populated and there is a population inversion between E_2 and E_1. (d) A random photon of energy $h\upsilon_{21} = E_2\text{-}E_1$ can initiate stimulated emission. Photons from this stimulated emission can themselves further stimulate emissions leading to an avalanche of stimulated emissions and coherent photons being emtitted.

Fig 3.40

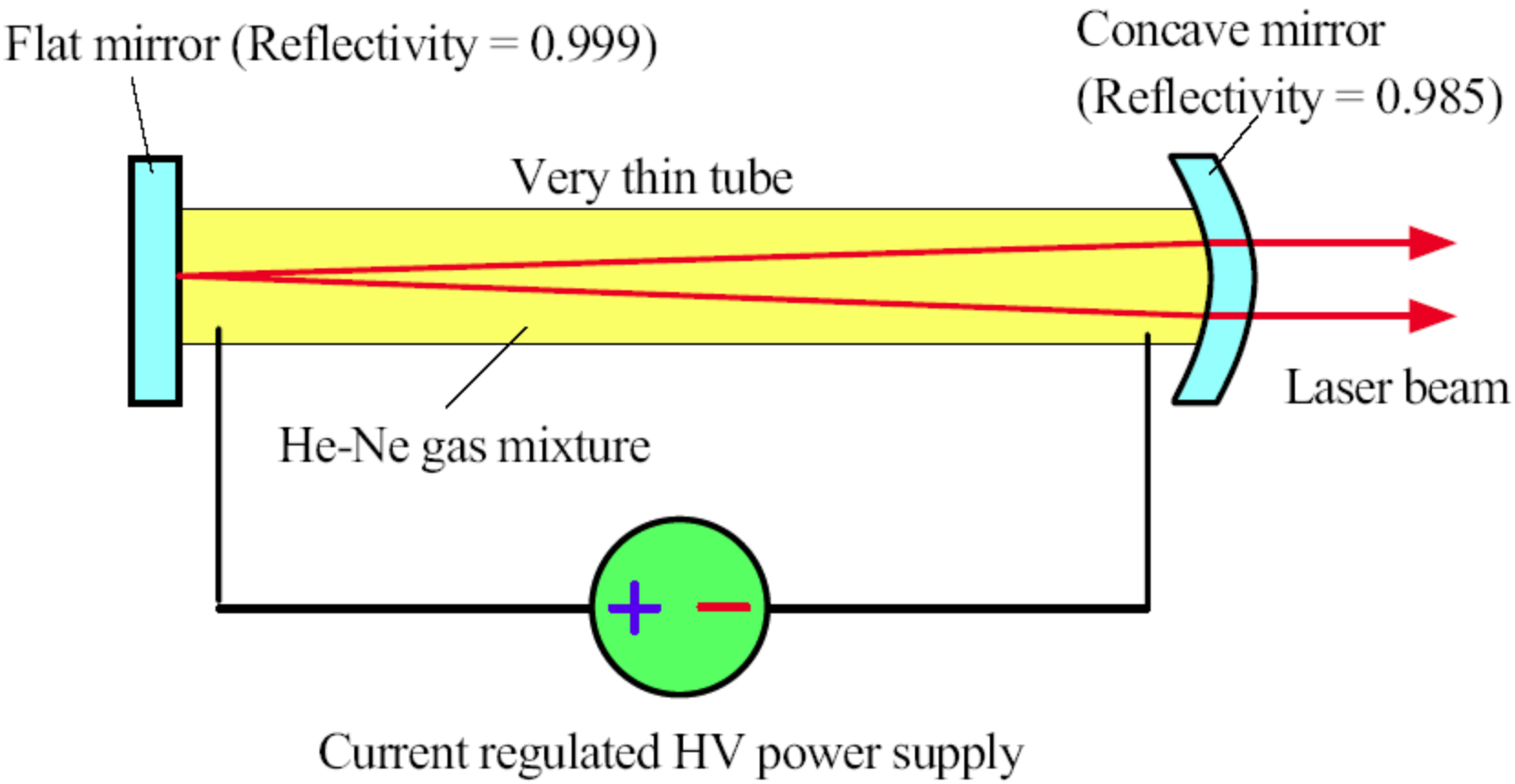

Schematic illustration of the HeNe laser.

Fig 3.41

A modern stabilized HeNe laser.
| SOURCE: Courtesy of Melles Griot.

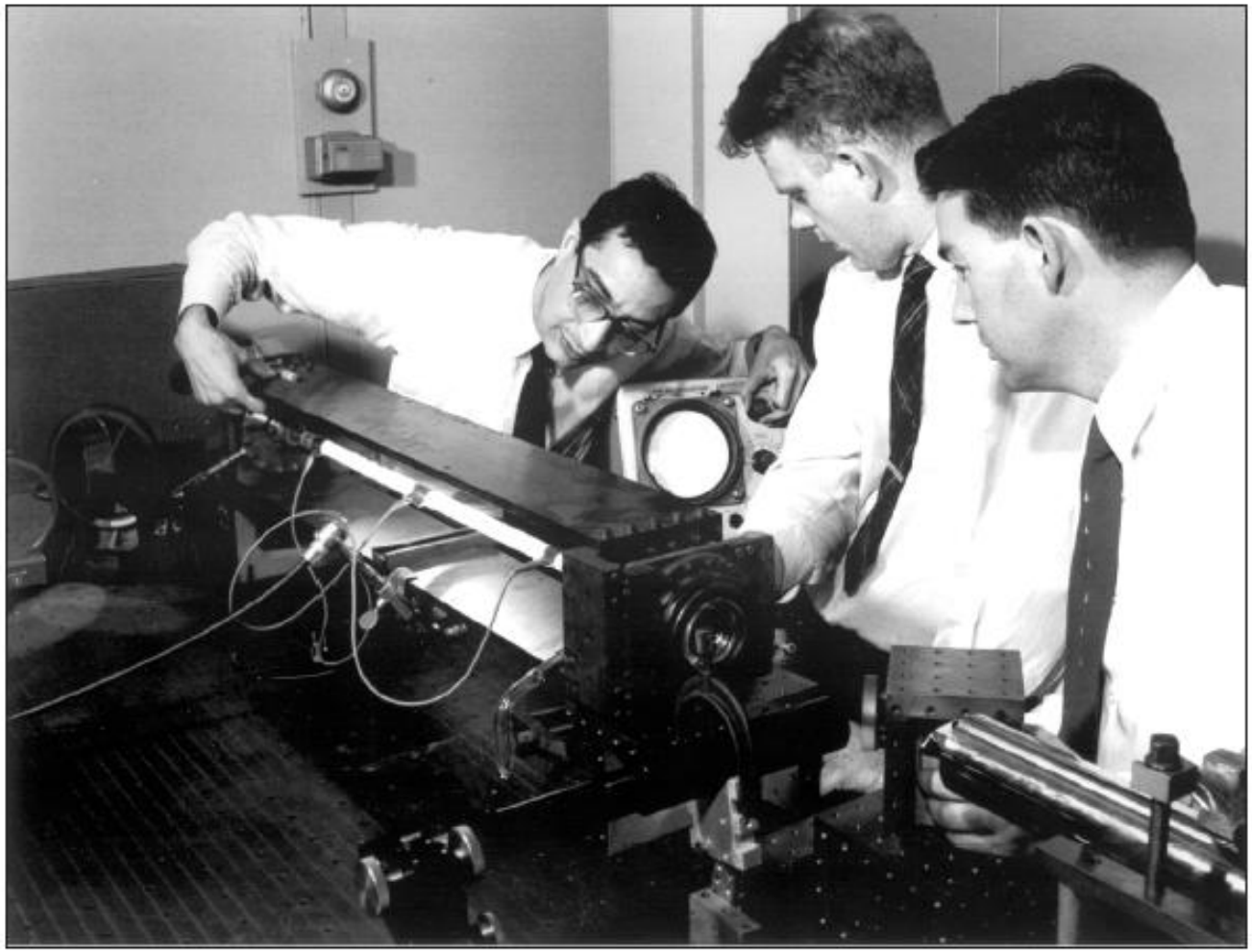

Ali Javan and his associates William Bennett Jr. and Donald Herriott at Bell Labs were first to successfully demonstrate a continuous wave (cw) helium-neon laser operation (1960).
| SOURCE: Courtesy of Bell Labs, Lucent Technologies.

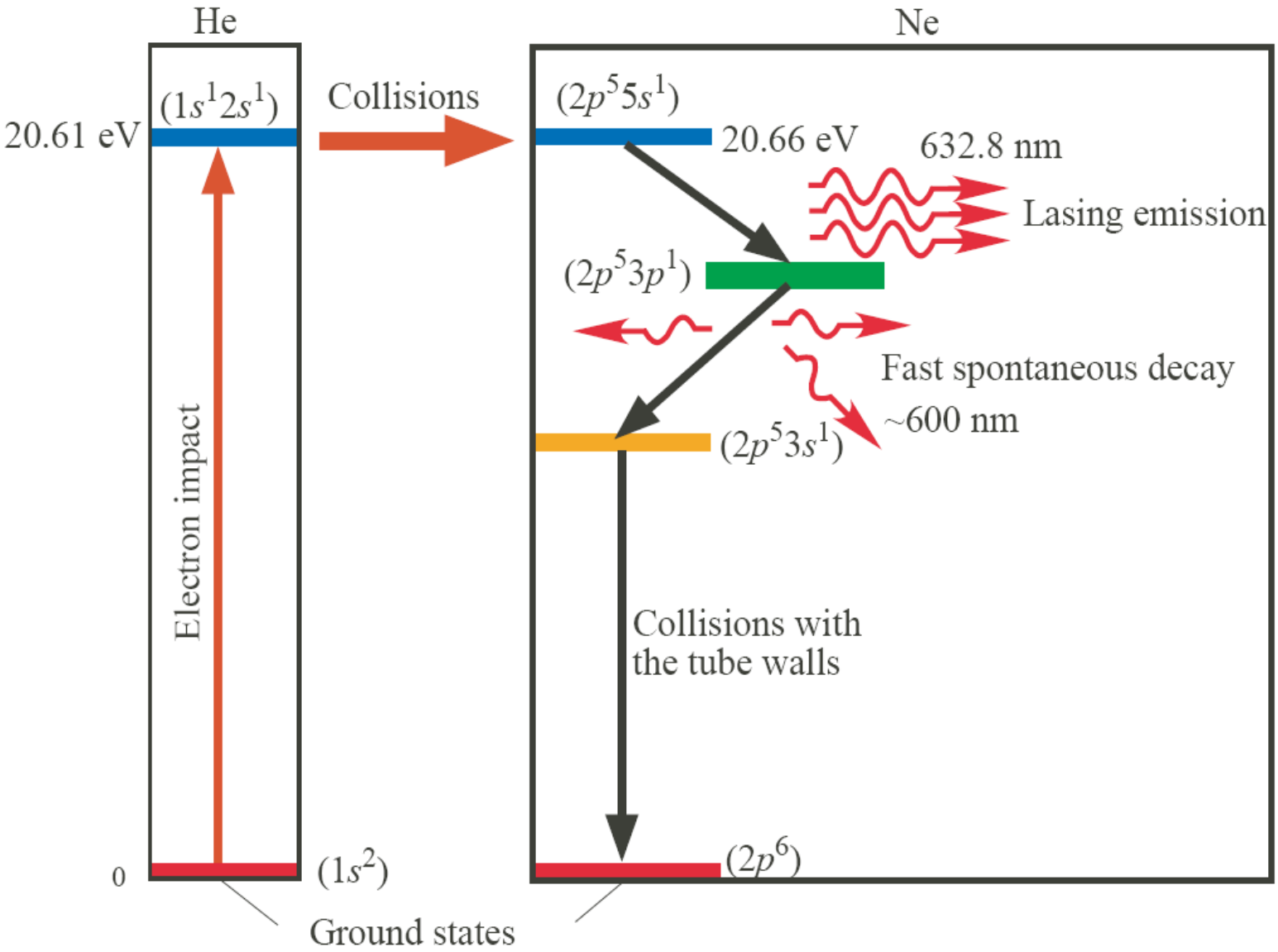

The principle of operation of the HeNe laser. Important HeNe laser energy levels (for 632.8 nm emission).

Fig 3.42

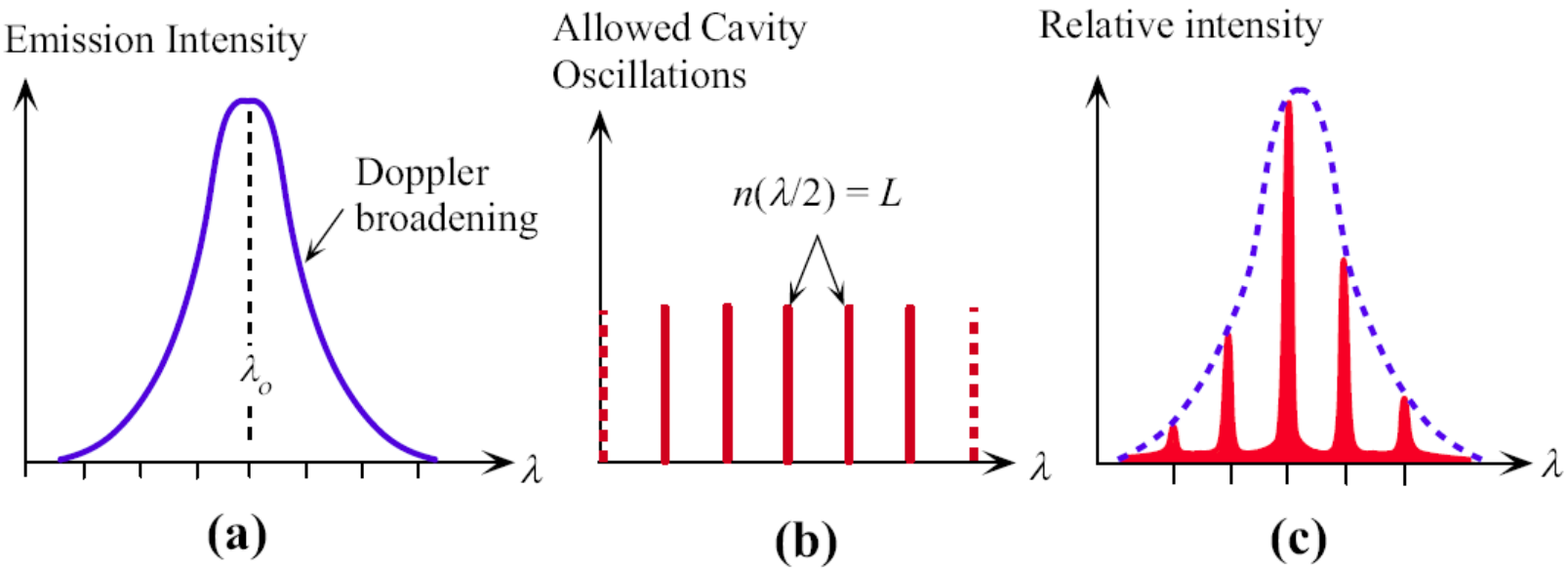

(a) Doppler-broadened emission versus wavelength characteristics of the lasing medium.
(b) Allowed oscillations and their wavelengths within the optical cavity.
(c) The output spectrum is determined by satisfying (a) and (b) simultaneously.

Fig 3.43

Laser Output Spectrum

Doppler effect: The observed photon frequency depends on whether the Ne atom is moving towards ($+v_x$) or away ($-v_x$) from the observer

$$\nu_2 = \nu_0\left(1+\frac{v_x}{c}\right) \qquad \nu_1 = \nu_0\left(1-\frac{v_x}{c}\right)$$

Frequency width of the output spectrum is approximately $\upsilon_2 - \upsilon_1$

$$\Delta\nu = \frac{2\nu_0 v_x}{c}$$

Laser cavity modes: Only certain wavelengths are allowed to exist within the optical cavity L. If n is an integer, the allowed wavelength λ is

$$n\left(\frac{\lambda}{2}\right) = L$$

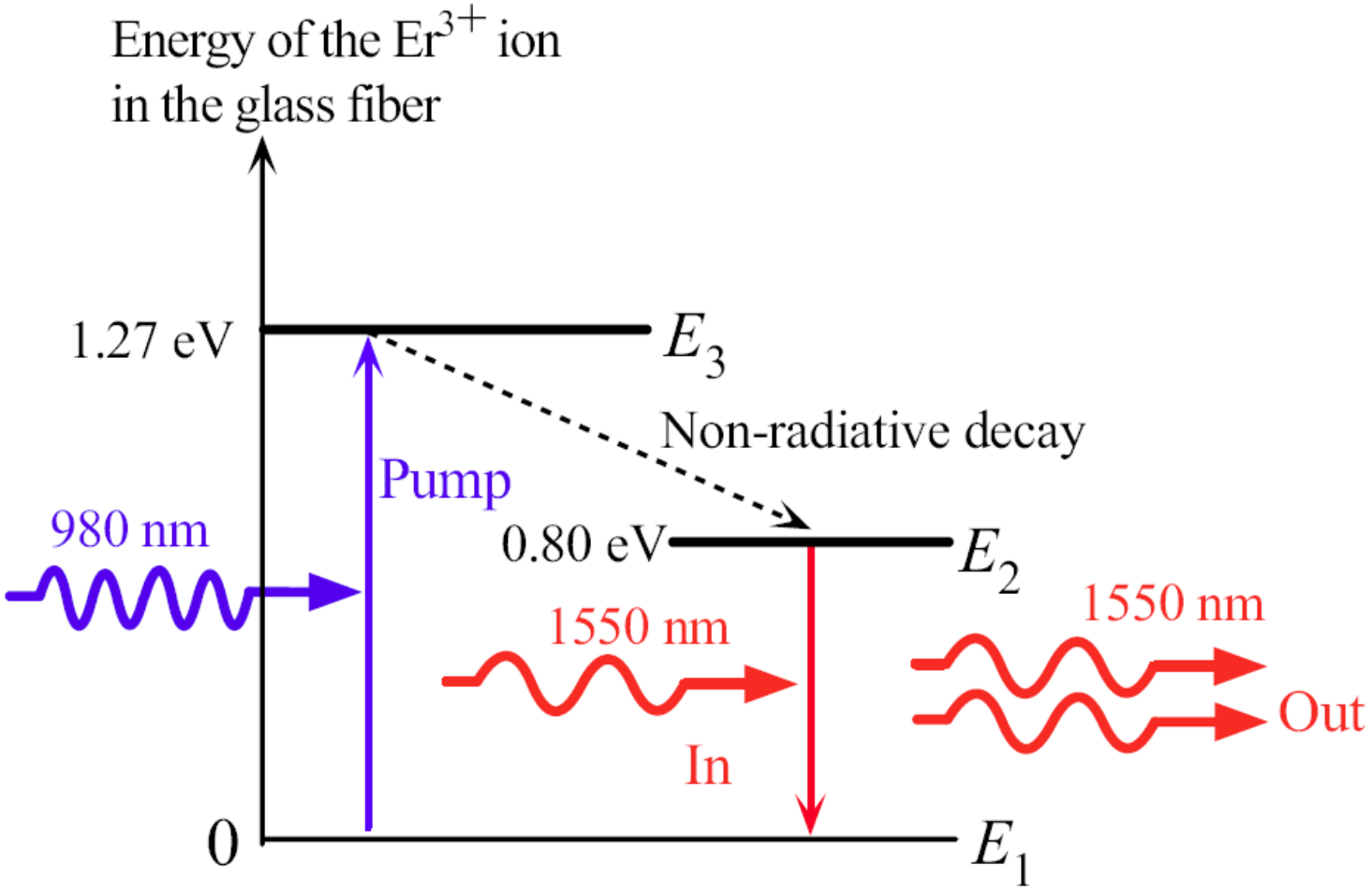

Energy diagram for the Er3+ ion in the glass fiber medium and light amplification by Stimulated emission from E2 to E1.
Dashed arrows indicate radiationless transitions (energy emission by lattice vibrations).

Fig 3.44

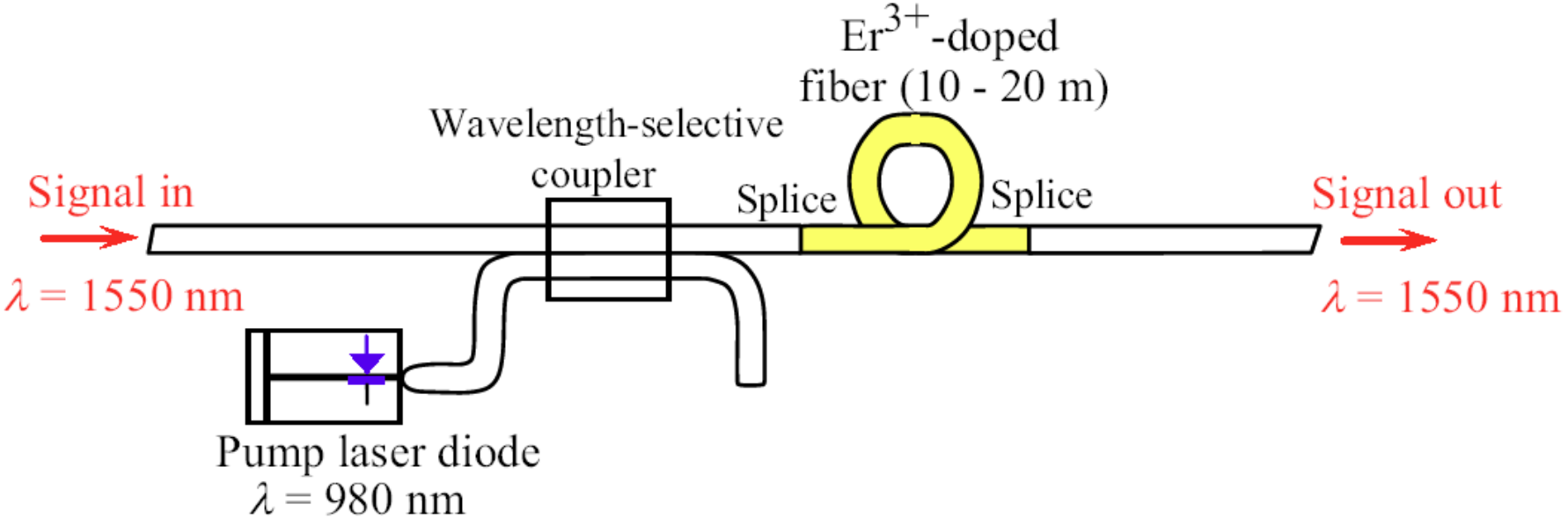

A simplified schematic illustration of an EDFA (optical amplifier). The erbium-ion doped fiber is pumped by feeding the light from a laser pump diode, through a coupler, into the erbium ion doped fiber.

Fig 3.45

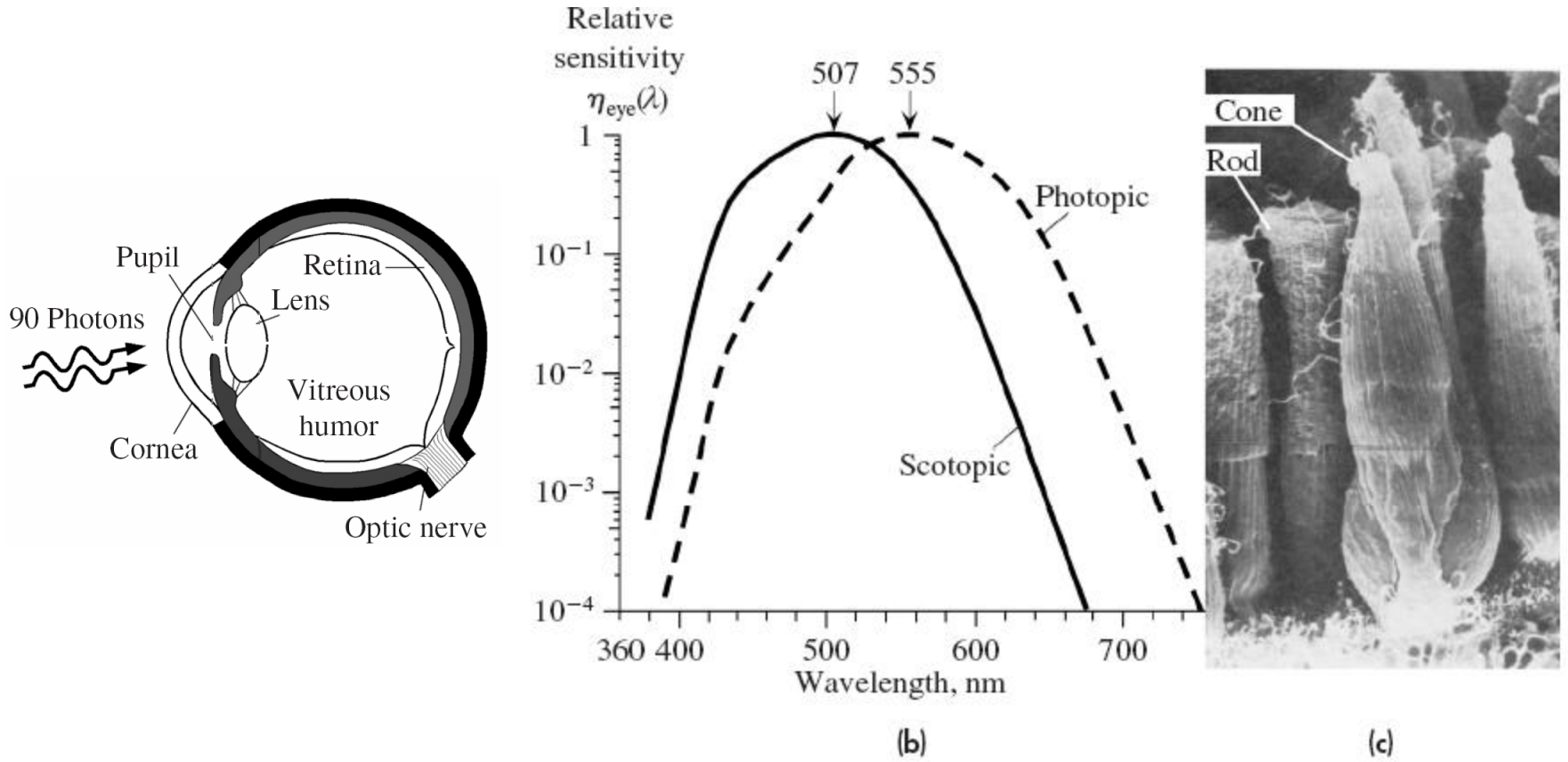

(a) The retina in the eye has photoreceptors that can sense the incident photons on them and hence provide necessary visual perception signals. It has been estimated that for minimum visual perception there must be roughly 90 photons falling on the cornea of the eye. (b) The wavelength dependence of the relative efficiency $\eta_{eye}(\lambda)$ of the eye is different for daylight vision, or *photopic* vision (involves mainly cones), and for vision under dimmed light, (or *scotopic* vision represents the dark-adapted eye, and involves rods). (c) SEM photo of rods and cones in the retina.
SOURCE: Dr. Frank Werblin, University of California, Berkeley.

Fig 3.46

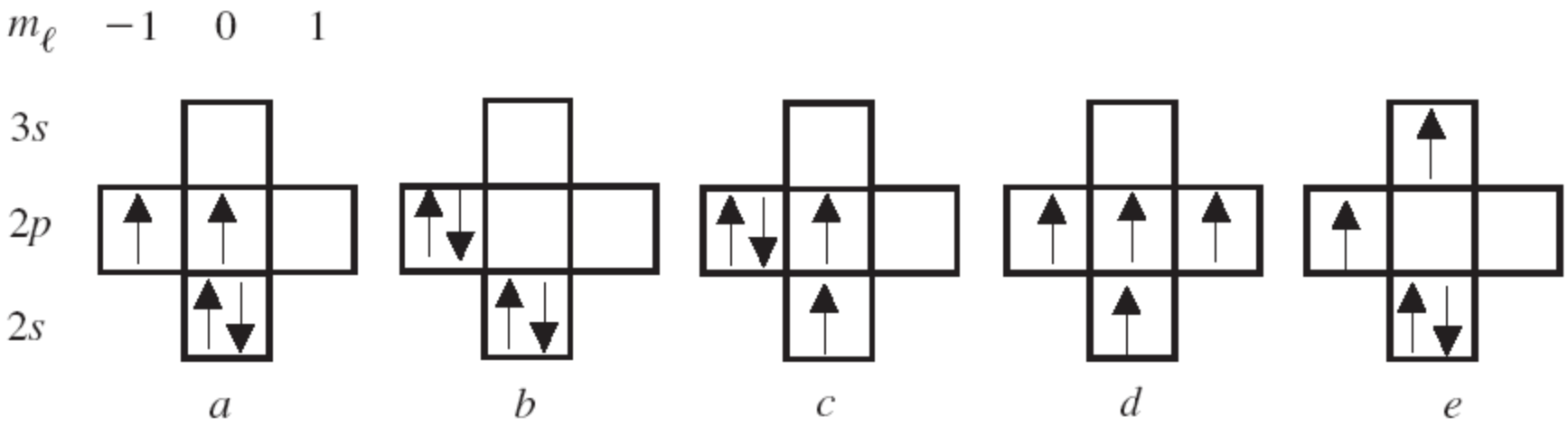

Some possible states of the carbon atom, not in any particular order.

Fig 3.47